Evolutionary history of two rare endemic conifer species from the eastern Qinghai-Tibet plateau

Article type: Original Article

Title:

Evolutionary history of two rare endemic conifer species from the eastern Qinghai-Tibet Plateau

Jibin Miao[1,2†], Perla Farhat[1,3†], Wentao Wang[1†], Markus Ruhsam[4], Richard Milne[5], Heng Yang[1], Sonam Tso[2], Jialiang Li[1], Jingjing Xu[1], Lars Opgenoorth[6], Georg Miehe[6], Kangshan Mao[1,2]*

Affiliation:

[1]Key Laboratory of Bio-Resource and Eco-Environment of Ministry of Education, College of Life Sciences, State Key Laboratory of Hydraulics and Mountain River Engineering, Sichuan University, Chengdu 610065, Sichuan, P.R. China;

[2]College of Science, Tibet University, Lhasa 850000, P.R. China;

[3]CEITEC–Central European Institute of Technology, Masaryk University, Kamenice 5, 625 00 Brno, Czech Republic

[4]Royal Botanic Garden Edinburgh, 20A Inverleith Row, Edinburgh EH3 5LR, UK;

[5]Institute of Molecular Plant Sciences, The University of Edinburgh, Edinburgh EH9 3JH, UK;

[6]Faculty of Biology and Geology, University of Marburg, 35032 Marburg, Germany.

[†]These authors contributed equally to this work.

Running title: Evolutionary history of two rare conifers from the Qinghai-Tibet Plateau

*For correspondence: maokangshan@scu.edu.cn or maokangshan@163.com.

ABSTRACT

Background and Aims Understanding the population genetics and evolutionary history of endangered species is urgently needed in an era of accelerated biodiversity loss. This knowledge is most important for regions with high endemism that are ecologically vulnerable, such as the Qinghai-Tibet Plateau (QTP).

Methods The genetic variation of 84 juniper trees from six populations of *Juniperus microsperma* and one population of *Juniperus erectopatens*, two narrow endemic junipers from the QTP that are sister to each other, was surveyed using RNA-seq data. Coalescent-based analyses were used to test speciation, migration, and demographic scenarios. Furthermore, positively selected and climate-associated genes were identified, and the genetic load was assessed for both species.

Key Results Analyses of 149,052 single nucleotide polymorphisms showed that the two species are well-differentiated and monophyletic. They diverged around the late Pliocene, but interspecific gene flow continued until the Last Glacial Maximum. Demographic reconstruction by Stairway Plot detected two severe bottlenecks for *J. microsperma* and only one bottleneck for *J. erectopatens*. The identified positive selected genes and climate-associated genes revealed habitat adaptation of the two species. Furthermore, although *J. microsperma* had a much wider geographical distribution than *J. erectopatens*, the former possesses lower genetic diversity and a higher genetic load than the latter.

Conclusions This study sheds light on the evolution of two endemic juniper species from the QTP and their responses to Quaternary climate fluctuations. Our findings emphasize the importance of speciation and demographic history reconstructions in the understanding of the current distribution pattern and genetic diversity of threatened species in mountainous regions.

Keywords: bottleneck event, conservation genomics, demographic history, effective population size, positively selected genes, habitat loss, *Juniperus microsperma*, *Juniperus erectopatens*, speciation history

INTRODUCTION

As a result of global climate change and the anthropogenic alteration of natural habitats (Dirzo *et al.*, 2014; Ceballos *et al.*, 2015; Cronk, 2016; Miraldo *et al.*, 2016; Ceballos *et al.*, 2017), numerous endangered species have experienced population declines (Allendorf *et al.*, 2010; Wang *et al.*, 2018) leading to higher than expected extinction rates (Barnosky *et al.*, 2011).Therefore, conservation genetic and ecological studies that aim to minimize the loss of rare species and maximize conservation efforts are urgently required (Harrisson *et al.*, 2014; Hamabata *et al.*, 2019, Segelbacher *et al.*, 2010; Casas-Marce *et al.*, 2013; Garner *et al.*, 2016). Habitat loss is often the primary factor that causes fragmentation of rare species resulting in small and isolated populations over short evolutionary time scales (Frankham, 2005; Hung *et al.*, 2014; Rogers and Slatkin, 2017). This may lead to reduced genetic diversity due to the more pronounced effects of genetic drift in small and isolated populations (Keller and Waller, 2002; Spielman *et al.*, 2004; Jacquemyn *et al.*, 2009). In general, threatened species tend to have low genetic diversity (Spielman *et al.*, 2004; Allendorf *et al.*, 2010), which increases the extinction risk (Saccheri *et al.*, 1998; Frankham, 2005). Therefore, it is crucial to understand how past events have shaped the demographic history of a species if we want to make predictions about how populations may respond to the future challenges (Ellegren and Galtier, 2016; Fan *et al.*, 2018). A key event in demographic histories is the fast reduction and subsequent increasement of the effective population size (N_e), usually known as a genetic bottleneck (Tajima, 1989*a*). This often negatively impacts the viability of a species through the loss of genetic diversity and various stochastic demographic processes (Frankham *et al.*, 1999; Frankham, 2005; Lima *et al.*, 2017). Therefore, knowledge of bottleneck events in the evolutionary history of a species, and of current levels of genetic diversity, are of critical importance when designing conservation and management strategies.

The Qinghai Tibet Plateau (QTP) *sensu lato*, especially its eastern and southern regions, holds tremendous biodiversity due to past geological and climatic changes (Wang *et al.*, 2007; Favre *et al.*, 2015; Fu *et al.*, 2020; Spicer *et al*., 2020). It is one of the most important alpine biodiversity hotspots in the world and a natural laboratory for evolutionary studies (Wen *et al.*, 2014; Huang *et al.*, 2018). Diverse habitats and ecological niches generated by the uplift of mountains (Rahbek *et al.*, 2019; Spicer *et al*., 2020) have promoted speciation (Liu *et al.*, 2013; Rahbek *et al.*, 2019) via allopatric and ecological speciation. Furthermore, the extensive oscillations of the climate on the QTP during the Quaternary led to repeated cycles of climate-driven changes of habitats, which promoted hybrid speciation as well as extinction over a short period of time (Fjeldså, 1994; Mosbrugger *et al.*, 2018; Nevado *et al.*, 2018; Muellner-Riehl, 2019; Rahbek *et al.*, 2019). The QTP contains about 9,000-12,000 species of plants (in about 1,500 genera), out of which more than 20% are endemic (Liu *et al.*, 2014; Wen *et al.*, 2014; Zhang *et al.*, 2016). Many of these endemic plant species are listed as rare and/or endangered (Duan and Liu, 2006; Liu *et al.*, 2011; Liu *et al.*, 2013; Wang and Li, 2016; Fu *et al.*, 2019), and face a high risk of extinction (López-Pujol *et al.*, 2011; Liu *et al.*, 2014) due to global warming and increased human activities on the QTP (He *et al.*, 2005; Diffenbaugh and Giorgi, 2012).

Conservation genomics has been applied to a number of endangered species which provided insight into the genetic diversity and evolutionary history of these species leading to informed and effective conservation and management plans (O'Brien, 1994; Pautasso, 2009; Allendorf *et al.*, 2010; Ouborg *et al.*, 2010; Segelbacher *et al.*, 2010). Unfortunately, such studies are lacking for endangered conifers on the QTP, despite their ecological importance. Here, we aim to unravel the evolutionary history of two rare endemic conifers, *Juniperus microsperma* (Cheng & L. K. Fu) R. P. Adams and *Juniperus erectopatens* (Cheng & L. K. Fu) R. P. Adams, in the eastern QTP (Adams

and Schwarzbach, 2013; Adams, 2014; Shang *et al.*, 2015; Xu *et al.*, 2019). *Juniperus microsperma* and *J. erectopatens* have slender leaves and irregular globose glaucous seed cones of similar size but differ in the number of seeds per cone [(1-)2-seeded vs. 1 seeded, respectively] and branchlet morphology (ascending vs. largely pendulous, respectively) (Adams, 2014). Although *J. microsperma* is the closest relative of *J. erectopatens* (Adams and Schwarzbach, 2013), they occur in areas ca. 800 km apart (Adams, 2014; Xu *et al.*, 2019). According to our field surveys, these two species are very rare. *Juniperus microsperma* is currently only found in the Parlung Zangbo Valley, Bomi County, southeastern QTP (Adams, 2014; Shang *et al.*, 2015) and *J. erectopatens* only occurs in one wooded area of approximately 2 km^2 at Anhong, Songpan, Sichuan, China (Adams, 2014; Xu *et al.*, 2019). Previous studies of these two species were limited to a small number of SNPs or indels from chloroplast and nuclear DNA markers (Shang *et al.*, 2015; Xu *et al.*, 2019), which might not reflect the genome-wide genetic variation. Due to recent advances in molecular biology technologies, genome-wide data can be rapidly generated by high-throughput sequencing (Ellegren, 2014; Goodwin *et al.*, 2016; Todd *et al.*, 2016; Fuentes-Pardo and Ruzzante, 2017) and analyzed using various bioinformatic tools (Ouborg *et al.*, 2010; Hamabata *et al.*, 2019).

Here, we employed high-throughput sequencing to detect the evolutionary history and its influence on the genetic diversity of two rare and closely related juniper trees, *J. microsperma* and *J. erectopatens*. Specifically, we aimed to address the following questions: (1) What is the pattern of genetic diversity and genetic load in *J. microsperma* and *J. erectopatens*? (2) When did these two species diverge from their most recent ancestor and what biogeographic history did they experience? (3) Which model of demographic history best explains the current genetic diversity? (4) How did orogeny events and climatic changes affect the evolutionary history of *J. microsperma*

and *J. erectopatens*? (5) Did habitat adaptation play a role during the evolution of the two species? Answering these questions will shed light on the conservation genomics and evolutionary history of QTP endemics as well as threatened plant species that occur in other mountainous regions all over the world.

MATERIALS AND METHODS

Sampling and RNA sequencing

Leaf samples were collected from a total of 84 mature individuals comprising 56 from *Juniperus microsperma* and 28 from *J. erectopatens*. The distance between sampled trees was more than 50 meters (Table 1 and Supplementary Data Table S1; Fig. 1C). In addition, 15 trees of *J. sabina* L. and five trees of *J. saltuaria* Rehder & E.H. Wilson were sampled as outgroups for further analysis. Fresh leaves were frozen in liquid nitrogen immediately after picking and kept at -80 °C prior to the RNA extraction. Total RNA was extracted using the RNeasy Kit (Qiagen, Hilden, Germany) and TRIzol reagent (Invitrogen, Carlsbad, CA, USA). RNA purity was checked using NanoPhotometer® spectrophotometer (IMPLEN, CA, USA) and the RNA concentration was measured using Qubit® RNA Assay Kit in Qubit® 2.0 Fluorometer (Life Technologies, CA, USA). RNA integrity was assessed using the RNA Nano 6000 Assay Kit of the Agilent Bioanalyzer 2100 system (Agilent Technologies, CA, USA). Sequencing libraries were prepared using NEBNext® Ultra™ RNA Library Prep Kit for Illumina® (NEB, USA) following standard RNA-seq methodology. After the above steps, 150-bp paired-end raw reads were generated on an Illumina Hiseq PE150 platform (Novogene, Beijing).

Read trimming and transcriptome de novo assembly

We used Trimmomatic ver.0.36 (Bolger *et al.*, 2014) to trim and filter Illumina raw reads, during which adapter sequences, poly-N and low-quality reads (Q < 30) were discarded. Filtered reads from one *J. microsperma* individual were assembled into contigs using Trinity ver.2.8.4 (Grabherr *et al.*, 2011) with default parameters. To obtain high-quality contigs, sequences were aligned to the microbial genome database (MBGDhttp://mbgd.genome.ad.jp/; Uchiyama *et al.*, 2009) via BLASTN ver.2.7.1 (Altschul *et al.*, 1997) and sequences with more than 90% similarity were discarded. CD-HIT ver.4.6.8 (Li and Godzik, 2006) was used to remove redundant sequences of assembled contigs with a threshold value of 0.99. Transcripts less than 200 bp were removed and the longest transcripts were selected in case of alternative splicing. Finally, 61,700 contiguous expressed sequences were obtained as the reference transcriptome.

Read mapping and variant calling

High-quality reads of *J. microsperma* and *J. erectopatens* individuals were aligned to the reference transcriptome using BWA-MEM ver.0.7.17 (Li and Durbin, 2009) with default parameters. To identify the ancestral state of characters for these two species, and for the phylogenetic analysis, we mapped the reads of one *J. oxycedrus* L., one *J. phoenicea* L., 15 *J. sabina* and five *J. saltuaria* samples to the reference transcriptome. Transcriptome sequence data of *J. oxycedrus* and *J. phoenicea* were taken from Mao *et al.* (2019). SAMTOOLS ver.1.9 (Li *et al.*, 2009) was used to convert the Sequence Alignment/Map (SAM) files to the Binary Alignment/Map (BAM) files, followed by sorting of the BAM files. Duplicate reads were marked and excluded from further analysis using PICARDTOOLS ver.2.18.11 (https://github.com/broadinstitute/picard/). The local regions around indels were realigned using RealignerTargetCreator and IndelRealigner tools in GATK ver.3.8.1 (DePristo *et al.*, 2011). Variants calling were conducted using the 'mpileup'

168 command in SAMTOOLS ver.1.9 (Li *et al.*, 2009) with parameters "-t AD,ADF,ADR,DP,SP -Q
169 20 -q 20".

170 To obtain a high-quality SNP set, we filtered those sites with mapping quality <30 and removed
171 indels within a 5bp window. Sites with coverage depth (DP) <10 were considered as missing for
172 each sample and SNPs with >50% of missing bases within either species were excluded. In
173 addition, we used VCFTOOLS ver. 0.1.15 (Danecek *et al.*, 2011) to remove variant sites which
174 differed significantly from Hardy-Weinberg equilibrium ($P < 0.001$) or which had a minimum
175 allele frequency of <0.05 to reduce the false discovery rate. In addition, we calculated the number
176 of shared and species-specific SNPs of *J. microsperma* and *J. erectopatens*.

177 The SNP dataset was used for population genetic and phylogenetic analyses, demographic
178 reconstruction, gene flow estimation, and the detection of environment-associated loci. In
179 parallel, we generated a gene sequence dataset to identify positively selected genes and the GO
180 annotation.

181

182 ***Population genetic and phylogenetic analysis***

183 The genetic structure of the two species was examined using a Bayesian Clustering
184 (ADMIXTURE) and principal component analysis (PCA). The SNP variant calling format was
185 converted into binary ped format for downstream analysis using VCFTOOLS ver.0.1.15. We used
186 PLINK ver.1.90 (Purcell *et al.*, 2007) to remove the linkage disequilibrium (LD) sites with
187 parameters "--indep-pairwise 50 10 0.4". The software ADMIXTURE ver.1.3.0 (Alexander and
188 Lange, 2011) was used to estimate the most likely number of distinct genetic clusters (K) by
189 varying K from 1 to 10 and by computing the parameters' maximum likelihood estimates. Twenty
190 independent replicates were run for each K to calculate the cross-validation errors. The optimal K

was indicated by the lowest cross-validation error. In addition, the PCA was performed via the SMARTPCA module in the software EIGENSOFT ver.7.2.1 (Price *et al.*, 2006).

For the phylogenetic analysis, we used a Perl script (Ru *et al.*, 2018) to convert filtered SNPs to concatenated sequences for each individual. A maximum likelihood (ML) phylogenetic tree for *J. microsperma* and *J. erectopatens* was reconstructed by RAxML ver.8.2.11 (Stamatakis, 2014) under the GTRGAMMA model using *J. oxycedrus* and *J. phoenicea* as outgroups. We ran 200 replicates to calculate bootstrap support values. The final phylogenetic tree was visualized using Figtree ver.1.4.3 (http://tree.bio.ed.ac.uk/software/figtree/).

To investigate the genetic differentiation between the two species, we calculated F_{ST} (Weir and Cockerham, 1984) using VCFTOOLS. Transcriptome-wide distribution of nucleotide diversity, θ_π (based on pairwise differences between sequences; Nei and Li, 1979) and θ_w (based on number of segregating sites between sequences; Watterson, 1975) were estimated using VCFTOOLS and the equations of Watterson (Watterson, 1975), respectively. Observed heterozygosity (H_o) and expected heterozygosity (H_e) was calculated for each population averaging across the individuals' total heterozygosity using an unpublished in-house Python script. The estimation of θ_π, θ_w, H_o, and H_e was performed on a subsample of seven individuals in Population 1, 2, 5, 6 and 7, and five individuals in Population 3 and 4 as there were only five individuals in these two populations (Table 1, S1). Also, Tajima's *D* (Tajima, 1989*b*) was calculated with VCFTOOLS for each of the two studied species. Negative values were set to zero followed by the mean value of genome-wide F_{ST} and the average number of nucleotide substitutions d_{XY} (Foote *et al.*, 2016) per locus was calculated using a Perl script (Ru *et al.*, 2018).

Demographic history and gene flow

Gene flow between *J. microsperma* and *J. erectopatens* was estimated via the detection of shared haplotypes between individuals of both species using a refined identity-by-descent (IBD) blocks analysis which was performed in Refined IBD with the parameters "window = 0.001 lod = 3.0 length = 0.0001 trim = 0.00001" (Browning and Browning, 2013).

We used the maximum-composite-likelihood approach based on the joint site frequency spectrum (SFS) implemented in *fastsimcoal2* (Excoffier *et al.*, 2013) to assess the fit of various demographic models and to infer the final optimal demographic scenario for *J. microsperma* and *J. erectopatens*. First, to minimize the effects of natural selection on demographic inference, we extracted a total of 1,050,559 four-fold degenerate synonymous (4DTV) sites from the SNP dataset which contained no missing bases across all individuals. A folded two-dimensional site frequency spectrum (2D-SFS) for *J. microsperma* and *J. erectopatens* was inferred based on 4DTV sites, and the joint SFS of each species were also inferred. The scripts from Ru *et al.* (2018) were used for extracting 4DTV sites and generating 2D-SFS, which was subsequently used to infer divergence time, bottleneck size and gene flow size between the two studied species. The mutation rate per generation was set to 9.7×10^{-9} and the generation time to 50 years following the parameters for Cupressaceae species in Li *et al.* (2012). Global ML estimates were derived from 50 independent runs, with 100,000 coalescent simulations and 40 likelihood maximization algorithm cycles. The Akaike information criterion (AIC; Akaike, 1974) was used to assess the relative fit of each model and the best fit with the lowest AIC was chosen. Ninety-five percent nonparametric bootstrap confidence intervals (CI) were constructed by sampling the 2D-SFS based on parameters of the preferred demographic scenario (Excoffier *et al.*, 2013).

In addition, we used Stairway Plot (Liu and Fu, 2015) to investigate the changes in effective population size over time for *J. microsperma* and *J. erectopatens* based on the joint SFS of each

237 species. Two hundred subsamples of 67% of all sites were created, the median value of the
238 estimation was used as a final output, and the 95% confidence interval of each value was produced
239 (Liu and Fu, 2015).
240
241 ***Detection of positive selection and GO annotation***
242 Coding and peptide sequences in the form of open reading frames (ORFs) were predicted for the
243 reference transcriptome using TRANSDECODER ver.5.5
244 (http://github.com/TransDecoder/TransDecoder/wiki/). To establish homology, the peptide
245 sequences in the ORF were blasted to the Swiss-Prot protein sequences database (Bairoch and
246 Apweiler, 2000) and the NR plant database (https://ftp.ncbi.nlm.nih.gov/blast/db/FASTA/) using
247 BLASTP ver.2.7.1 (Altschul *et al.*, 1997). We also used a Python script and idmapping.tb.gz
248 (ftp://ftp.pir.georgetown.edu/databases/idmapping) to determine gene functions according to the
249 Gene Ontology (GO) terms (Ashburner *et al.*, 2000) and to merge the results of the Swiss-Prot
250 database and the NR plant database searched for the final annotation.
251 The population branch statistic (PBS) analysis (Yi *et al.*, 2010) and the Hudson-Kreitman-
252 Aguadé (HKA) test were applied to detect candidate genes under positive selection within each of
253 the two target species, *J. microsperma* and *J. erectopatens*. Fifteen individuals of *J. sabina* were
254 used as the control group, and five individuals of *J. saltuaria* served as outgroup. We calculated
255 the population branch statistic for two triplets, *J. microsperma-J. sabina-J. saltuaria* and *J.*
256 *erectopatens-J. sabina-J. saltuaria* using the Perl script "PBS_test.pl" from Ma *et al.* (2019)
257 (https://github.com/mayz11/cypress). The F_{ST} value was calculated between the following
258 population pairs (a) the target population and the control population, (b) the target population and
259 outgroup, (c) the control population and outgroup.

We also used the custom Perl script "HKA_test.pl" from Ma *et al.* (2019) (https://github.com/mayz11/cypress) to carry out the HKA tests (Hudson *et al.*, 1987). We considered the number of polymorphic sites in the target population (*J. microsperma* or *J. erectopatens*) as A, and the number of fixed differences between the target populations and both the control group (*J. sabina*) and the outgroup (*J. saltuaria*) as B. The ratio of A/B for each unigene was compared to the transcriptome-wide average and the null hypothesis A (unigene)/B (unigene) = A (transcriptome-wide)/B(transcriptome-wide) was tested using Pearson's chi-square test for the 2 × 2 contingency table.

Unigenes with the highest 10% of the population branch statistic with a significant *P*-value (<0.05) for the Hudson-Kreitman-Aguadé test were considered as candidate genes under positive selection in *J. microsperma* or *J. erectopatens*. GO enrichment analysis was conducted using TBtools (Chen *et al.*, 2020). Fisher's exact test was employed to examine the significance of the GO enrichment in which the corrected *P*-values < 0.05 were considered significant.

Detection of environment-associated loci

Latent Factor Mixed Models (LFMM) (Frichot et al. 2013) were used to measure the associations between SNPs and climatic gradients while accounting for underlying population structure. This method estimates allele-environment correlations between each SNP and each variable at a time. In LFMM, environmental variables are tested separately and introduced into each model as fixed effects. The number of latent factors (K) is included in the model as a covariate and the environmental gradients were not considered in the analysis (Frichot *et al.* 2013).

A total of 19 climate variables (Table S2, 1970-2000) were retrieved from WorldClim (https://www.worldclim.org/; Hijmans et al. 2005). We extracted the climate variables for each

population location using the R package DISMO (Hijmans et al. 2015). To avoid multicollinearity, we discarded variables that were highly correlated (Pearson's $r > 0.8$). The remaining subset of four uncorrelated BIOCLIM variables, including BIO3, BIO10, BIO17, and BIO19 were retained for further analysis. For each of the four uncorrelated BIOCLIM variables, we run five independent runs to simulate the correlation between SNPs and climate factors, using 100,000 iterations and 50,000 burn-in with a latent factor of K = 2, according to the results of ADMIXTURE, in the R package LEA (Frichot and François 2015). The five separate runs had nearly similar |z|-scores. Second, we calculated the mean |z|-scores and considered a false discovery rate (FDR) of 0.05 to be significant. Finally, we conducted a GO enrichment analysis.

Assessment of genetic load

Nucleotide diversity (θ_π) of zero-fold and four-fold degenerate sites, as well as the ratio between the two indices, were calculated within coding regions based on the annotation of *J. microsperma* (Marsden *et al*., 2016; Petit, Hu, & Dick, 2008; Wang *et al*., 2021). The zero-fold and four-fold degenerate sites were identified by iterating across all four possible bases at each site along a transcript and recording the changes in the resulting amino acid using the Perl script (https://github.com/wk8910/bio_tools/blob/master/00.scripts/get_0fold-4fold_sites.pl). Sites were classified as zero-fold degenerate when the four different bases resulted in four different amino acids. However, sites were considered as four-fold degenerate when no changes in amino acids were detected. Besides, we estimated the θ_π(0-fold)/θ_π(4-fold) ratios for each species to test the accumulation of missense mutations (Wang *et al*., 2021).

RESULTS

Reference transcriptome assembly and SNPs calling

The assembled reference transcriptome of *J. microsperma* contained 61,700 unigenes with an average length of 907 bp and a contig N50 equaling 1,793 bp. After removing low-quality Illumina sequences, 3.6 Gb of reads remained for the assayed 84 samples (56 from *J. microsperma* and 28 from *J. erectopatens*). Following the alignment of the transcriptome reads from all individuals to the reference transcriptome and undertaking stringent quality filtering with 50% missing data (SNP) per species, we identified 149,052 high-quality SNPs across all studied individuals. A total of 81,775 SNPs were shared between *J. microsperma* and *J. erectopatens*, and the number of species-specific SNPs were 20,758 and 46,519, respectively (Supplementary Data Fig. S1).

Population genetic structure and genetic diversity

Our phylogenetic analysis based on 149,052 SNPs showed that samples belonging to each species, *J. microsperma* and *J. erectopatens*, were clustered into a separate monophyletic clade (Fig. 2B). Principal component analysis (PCA) based on SNPs also distinguished the two species along PC1 (variance explained = 15.8%; Figs 2C and D). Furthermore, analysis of population genetic structure clearly assigned the individuals of *J. microsperma* and *J. erectopatens* into a species-specific group when $K = 2$, which was estimated to be the optimal value of K (Fig. 1C and Supplementary Data Figs S2 and S3). In addition, the two species were well differentiated based on F_{ST} (0.233) and d_{XY} (0.319) values (Table 2; Supplementary Data Fig. S4).

The transcriptome-wide average values for both indicators of nucleotide diversity, θ_π and θ_w, were higher for *J. erectopatens* ($\theta_\pi = 0.00222$, $\theta_w = 0.00139$) than for *J. microsperma* ($\theta_\pi = 0.00129$, $\theta_w = 0.00099$) (Table 2). Observed (H_o) and expected (H_e) heterozygosity were lower in *J. microsperma* (H_o=0.198, H_e=0.169) compared to *J. erectopatens* (H_o=0.369, H_e=0.289; Table 2).

To avoid a potential bias due to different sample numbers per population, we selected a small subset of individuals (seven from five populations, and five from two populations) for measurements of nucleotide diversity parameters. All six populations of *J. micropserma* presented values of θ_π, θ_w, H_o and H_e lower than the single population of *J. erectopatens* (Supplementary Data Table S3). Tajima's *D* indicated that a large number of alleles with medium frequency were retained in *J. microsperma* (*D* =0.68151) and *J. erectopatens* (*D* =1.50340, Table 2), suggesting that both species may have experienced population bottleneck(s) and/or balanced selection in their population evolutionary history.

Juniperus microsperma had relatively lower θ_π compared with *J. erectopatens* in both 0-fold and 4-fold sites (Fig. 3). The $\theta_{\pi\ (0\text{-fold degeneration variants})}/\theta_{\pi\ (4\text{-fold degeneration variants})}$ ratio for each species was higher for *J. microsperma* than it was for *J. erectopatens* (Figure 3c), suggesting that *J. microsperma* accumulated more missense mutations and possesses a higher genetic load.

Gene flow and demographic history

To detect whether gene flow existed between *J. microsperma* and *J. erectopatens*, we identified shared haplotypes between these two species using the refined identical-by-descent (IBD) approach (Browning and Browning, 2013). Pairwise comparisons between individuals showed that haplotype sharing was common between *J. microsperma* and *J. erectopatens* (131 out of 1568 pairwise comparisons indicated haplotype sharing; Fig. 4). All shared haplotypes were short in length, due to the relatively short length of unigenes in the transcriptome dataset. However, they were of sufficient length to reveal intra- and inter-specific gene flow (Ma *et al.*, 2019). In summary, these results indicated that historical gene flow has occurred between *J. microsperma* and *J. erectopatens*.

352 The timing of speciation, population contraction(s) and expansion(s), and levels of gene flow
353 between the two species were estimated using coalescent-based simulations in *fastsimcoal2*
354 (Excoffier *et al.*, 2013). First, we established six demographic models for *J. microsperma* and *J.*
355 *erectopatens* covering a large range of demographic possibilities (Supplementary Data Fig. S5
356 Model-A to Model-F). These six demographic models were identified as representative scenarios
357 based on the current population size and distribution of *J. microsperma* and *J. erectopatens*.
358 Besides, these models were representative of the demographic histories of QTP's rare conifers in
359 previous studies (Shang *et al.*, 2015; Xu *et al.*, 2019). AIC results favored for *J. microsperma* the
360 model where two sequential bottleneck events occurred, whereas for *J. erectopatens*, they favored
361 the model in which one bottleneck event took place (Supplementary Data Fig. S5). Based on these
362 preferred models, we merged the best suggested demographic scenarios to form the optimal model
363 for the demographic relationship between the two species. Because the bottleneck events detected
364 in the two species may have occurred in their common ancestor, we included in the models further
365 bottleneck events and divergence times. After comparing four models (Supplementary Data Fig.
366 S5 Model-1 to Model-4), Model-3 was shown to be the optimal one. This model suggested that *J.*
367 *microsperma* and *J. erectopatens* diverged from their common ancestor after the first bottleneck
368 event (Supplementary Data Fig. S5).
369 The best-fitting model (with minimum Akaike's weight value) containing 17 parameters
370 (Supplementary Data Tables S4 and S5; Fig. 5A), indicated that *J. microsperma* and *J.*
371 *erectopatens* diverged from each other approximately 3.31 million years ago (Mya) (95%
372 confidence interval (CI): 2.62-3.74 Mya; Supplementary Data Table S5; Fig. 5A). After
373 divergence, *J. microsperma* experienced one bottleneck event between 0.90 Mya (CI: 0.67-1.34
374 Mya) and 0.43 Mya (CI: 0.31-0.48 Mya) with a decrease in effective population size (N_e) from

62,831 (CI: 33,345-85,507) to 435 (CI: 124-2533). Later, the population size of *J. microsperma* increased to 12,920 (CI: 12,157-16,570) but failed to recover to the pre-bottleneck size (Fig. 5A; Supplementary Data Table S5). In contrast, *J. erectopatens* only experienced one population contraction at approximately 76 Kya (CI: 51-124 Kya), with a decrease in N_e from 88,821 (CI: 63,250-95,861) to 6,638 (CI: 6,207-9,243) (Supplementary Data Table S5; Fig. 5A). After divergence, the gene flow between the two species persisted until approximately 22 Kya (CI: 16-35 Kya) and was slightly higher from *J. erectopatens* to *J. microsperma* than in the opposite direction (8.76×10^{-05} vs. 4.17×10^{-05}) (Supplementary Data Table S5; Fig. 5A).

To obtain more robust interpretations of demographic history of these two species, we used a Stairway Plot analysis. This analysis showed that the effective population size of *J. microsperma* declined sharply at approximately 1.0 Mya, and then quickly arose about 0.8 Mya (Fig. 5B). After this, N_e declined again around 40 Kya and increased to its current level at about 13 Kya (Fig. 5B), suggesting that *J. microsperma* experienced two severe population bottleneck events. The N_e of *J. erectopatens* displayed a slow decline around approximately 70 - 100 Kya and then expanded rapidly around 3 - 5 Kya (Fig. 5B). This indicates that *J. erectopatens* experienced a single bottleneck event that last longer, yet less severe and less recovered than the (roughly) contemporary bottleneck experienced by *J. microsperma*.

Detection of positive selection genes

We found a total of 24,847 coding peptide sequences from the reference transcriptome. Of these, 17,883 and 18,056 peptide sequences were annotated using the Swiss-prot database and the NR plant database, respectively. After merging the outputs from both databases, a total of 19,786 peptide sequences were annotated.

To explore the genetic basis of possible adaptation in *J. microsperma* and *J. erectopatens*, PBS and HKA tests were conducted to identify genes under positive selection within the two species. In total, 183 and 85 positively selected candidate genes were identified within *J. microsperma* and *J. erectopatens*, respectively. The over-represented GO terms identified by GO enrichment analysis for positively selected candidate genes within *J. microsperma* included aerenchyma formation, positive regulation of salicylic acid-mediated signaling pathway, response to decreased oxygen levels, and the terpenoid biosynthetic process (Supplementary Data Table S6). In contrast, no significant GO enrichment category was detected for the positively selected candidate genes within *J. erectopatens* (Supplementary Data Table S7). Nevertheless, four marginally significant GO enrichment categories were detected, including glycosyl and organonitrogen compound biosynthetic process, antiporter and secondary active transmembrane transporter activity ($0.07 < P < 0.08$; Supplementary Data Table S7).

Detection of environment-associated loci

We found that 18,723; 7,883; 10,118 and 9,799 SNPs were associated with the climate variables BIO3, BIO10, BIO17 and BIO19 (described above), respectively [false discovery rate (FDR)–corrected $P< 0.05$]. From the 2,127 SNPs associated with all four variables, we identified 49 categories of genes of various function detailed in the supplementary Table S8. Furthermore, six of these gene categories are involved in response to abiotic and biotic stimuli such as the immune system process, ethylene biosynthetic process, response to oxygen-containing compound, defense response to insect, response to stress, and response to hormone (Table 3).

DISCUSSION

Genetic differentiation and diversity of J. microsperma *and* J. erectopatens

All our population genomic analyses suggested that *J. microsperma* and *J. erectopatens* are well differentiated (Figs 2A, C and D). Similarly, the phylogenetic tree showed that all individuals of *J. microsperma* and *J. erectopatens* formed a monophyletic clade (Fig. 2B). This is consistent with the most recent phylogenetic study for *Juniperus* based on ITS and four chloroplast genes (Adams and Schwarzbach, 2013). Furthermore, the pairwise F_{ST} and $d_{\underline{XY}}$ values indicated moderate to high levels of genetic differentiation between these two species (Table 2; Supplementary Data Fig. S4).

In general, species that occupy a larger distribution range tend to possess higher levels of genetic variation than those with a smaller range and population size (O'Brien, 1994; Frankham, 1997). However, we detected a contrasting pattern for these two rare juniper species, because *J. erectopatens* occurs in a much smaller geographical area than *J. microsperma* (Fig. 1) and has twice the number of species-specific SNPs compared to *J. microsperma* (Supplementary Data Fig. S1). Furthermore, the nucleotide (θ) and gene diversity (H_e) of *J. erectopatens* were higher than those of *J. microsperma* (Table 2; Supplementary Data Table S3), suggesting higher levels of diversity in *J. erectopatens*. Interestingly, the nucleotide diversities of both *J. microsperma* (θ_π = 0.00129, θ_w = 0.00099) and *J. erectopatens* (θ_π = 0.00222, θ_w = 0.00139) found in this study were lower than those previously published for other conifer species. For example, θ_π = 0.0029 for *Cupressus gigantea* W.C.Cheng & L.K.Fu., θ_π = 0.0031 for *C. duclouxiana* Hickel (Ma *et al.*, 2019), θ_π = 0.00770 for *C. chengiana* S.Y.Hu (Li *et al.*, 2020*b*), θ_π = 0.00411 for *Picea likiangensis* (Franch) E.Pritz., θ_π = 0.00392 for *P. purpurea* Mast., and θ_π = 0.00392 for *P. wilsonii* Mast. (Ru *et al.*, 2018), whereas θ_w = 0.0144 for *C. gigantea* and θ_w = 0.0151 for *C. duclouxiana* (Ma *et al.*, 2019). Different factors may have contributed to the relatively low levels of genetic diversity of *J.*

444 *microsperma* and *J. erectopatens*, such as the evolutionary history and the current small population
445 sizes as indicated by the narrow geographical distribution of the two species. This is supported by
446 Tajima's D <0 (Table 2), which suggests that the two junipers have experienced bottlenecks or
447 balancing selection in their demographic history. Rare alleles are lost during such events, leading
448 to reduced diversity (Frankham *et al.*, 1999; Spielman *et al.*, 2004; Ellegren and Galtier, 2016).
449 Furthermore, the loss of rare alleles due to genetic drift is more pronounced when N_e is small,
450 further decreasing genetic diversity (Stoffel *et al.*, 2018; Hahn, 2019; Freeland, 2020). Hence, the
451 relatively small population sizes in both *J. microsperma* and *J. erectopatens* would also have
452 contributed to the low genetic diversity within these two species.
453
454 ***Contrasting range and diversity pattern reflects different demographic history***
455 Our demographic models using *fastsimcoal2* and Stairway Plot indicated that the two species
456 went through bottlenecks in the past. However, the results for each species were somewhat
457 contradictory between the two approaches as *J. microsperma* experienced one bottleneck
458 according to the *fastsimcoal2* analysis (Supplementary Data Table S4; Fig. 5A) and two according
459 to Stairway Plot (Fig. 5B). Similarly, although *J. erectopatens* had one bottleneck event in both
460 simulations, a modest population expansion was detected using Stairway Plot which was not
461 apparent using *fastsimcoal2* (Fig. 5B). Both methods rely on the (SNP) site frequency spectrum
462 (SFS) to infer the demographic history of species, however, the internal algorithm of each software
463 is different (Excoffier *et al.*, 2013; Liu and Fu, 2015). *Fastsimcoal2* uses a series of pre-defined
464 demographic models and a maximum likelihood approach to estimate the best fitting model
465 (Excoffier *et al.*, 2013), whereas Stairway Plot is a model-independent method that uses the
466 expected composite likelihood method (Liu and Fu, 2015). In our analyses, both methods detected

demographic events around or before the Last Glacial Period (LGP), yet Stairway Plot detected recent demographic events that *fastsimcoal2* did not (Fig. 5). Hence, the resolution of *fastsimcoal2* to recent demographic events may be less sensitive compared to Stairway Plot. However, it has been shown that despite these shortcomings a combination of the two approaches can reveal deeper insights into the demographic history of a species (Hansen *et al.*, 2018).

The key points which emerge from the demographic analyses are that during the Quaternary *J. microsperma* experienced considerable population bottleneck(s), which likely caused the current low levels of genetic diversity. One bottleneck occurred between 0.90–0.43 Mya (Supplementary Data Table S4; Fig. 5A), which corresponds to two of the most intense periods of glaciation on the QTP, i. e. the Xixiabangma Glaciation (1.2–0.8 Mya) and the Naynayxungla Glaciation (0.72–0.5 Mya) (Zheng *et al.*, 2002; Zhou *et al.*, 2011). During this bottleneck event, the N_e of *J. microsperma* shrank severely, from 62,831 to 435 and only recovered to ca. 1/5 of the pre-bottleneck size (12,920; Supplementary Data Table S4; Fig. 5A), which emphasizes the severity of this event. Another bottleneck might have occurred more recently between 13 to 40 Kya (Supplementary Data Table S4; Fig. 5B) which coincides with the LGM (Clark et al., 2009, Yokoyama et al., 2000), in which the population shrank and then expanded rapidly to nearly 100% of pre-bottleneck levels. These periods coincided with the Xixiabangma Glaciation and the Last Glacial Maximum (LGM; Yokoyama *et al.*, 2000; Clark *et al.*, 2009). The effective population size N_e of *J. microsperma* was reduced by 80-99% but recovered substantially after the event(s) to somewhere between 25% to nearly 100% of pre-bottleneck levels, depending on the demographic approach (Figure 5). Despite the substantially different estimates of the effective population sizes between the two approaches, the results are consistent in that *J. microsperma* experienced major population losses but was able to increase numbers significantly after the events. This is also

consistent with previous studies which showed that the periods with the most extensive glaciation and the Last Glacial Maximum have caused significant changes to the distribution and N_e of plants on the QTP (Sun *et al.*, 2014; Ren *et al.*, 2017; Chen *et al.*, 2019; Ma *et al.*, 2019; Feng *et al.*, 2020; Li *et al.*, 2020*a*; Li *et al.*, 2020*b*).

Unlike for *J. microsperma*, both methods indicated only a single population contraction event for *J. erectopatens*. This occurred around 100–70 Kya (depending on the method used) with a reduction in N_e between 81%-93% (Supplementary Data Table S4; Fig. 5A). This event coincided with the beginning of the Last Glacial Period (LGP) around 110 Kya (Thompson *et al.*, 1997) and is consistent with previous studies that also indicated that this glacial period affected the distribution of plants in the QTP (Wang *et al.*, 2009; Shimono *et al.*, 2010). After a considerable period of population size depression, *J. erectopatens* may have experienced a population expansion around 5-3 Kya when the climate became more stable (Yu *et al.*, 1997; Hou *et al.*, 2017) but this is only evident from the Stairway Plot analysis (Fig. 5B).

One unexpected result of this study was the lower level of (whole transcriptome-wide) genetic diversity in *J. microsperma* compared to *J. erectopatens*, despite the currently larger population size and distribution range of *J. microsperma*. The results from both demographic analyses suggested that *J. microsperma* had about a 30% smaller ancestral effective population size (N_{JM1}, Fig. 5) than *J. erectopatens* (N_{JE1}, Fig. 5). Therefore, it is likely that this also corresponds to an initially lower level of genetic diversity which was further reduced during one or even two bottleneck events (Fig. 5).

The contrasting demographic history of the two junipers may also be a reflection of the heterogeneity of changes in the local climate on the eastern QTP. Previous studies have shown that climate changes on the QTP affected the distribution and effective population size of plants (Ru *et*

al., 2016; Chen *et al.*, 2019; Ma *et al.*, 2019; Zhang *et al.*, 2019; Li *et al.*, 2020*b*). For example, species which occur in different regions on the QTP may have experienced a distinct demographic history due to different local climates and geographical factors (Owen and Dortch, 2014). *Juniperus microsperma* occurs in the deep river valley of the Parlung Zangpo around 3150-3350 m (Adams, 2014; Shang *et al.*, 2015), which is surrounded by numerous mountain peaks (> 5000 m) and modern glaciers (Zheng and Rutter, 1998; Yang *et al.*, 2010). In contrast, *J. erectopatens* occurs in the upper Minjiang river valley (Adams, 2014), where the local terrain is less rugged and is covered by fewer glaciers (Wang *et al.*, 2017). Hence, the expansion of local glaciers during colder periods (Zhou *et al.*, 2010) might have affected *J. microsperma* more severely, reducing its population size but permitting rapid expansion during warmer periods. This could be the reason why Stairway Plot identified two bottleneck events for *J. microsperma*, which coincide with two glacial periods on the QTP. Our results are in agreement with the geological evidence suggesting that the paleoclimatic changes in different regions on the QTP and the Himalayas may be driven by different factors. Indeed, while glaciers in some regions are likely to respond to the climate oscillations of the Northern Hemisphere, other regions may be more influenced by the southern Asian monsoon (Owen and Dortch, 2014).

Speciation history of the two junipers

The divergence time of *J. microsperma* and *J. erectopatens* was estimated to occur during Pliocene, at around 3.13 Mya (CI: 2.62-3.74 Mya) (Supplementary Data Table S4; Fig. 5A). A possible trigger for this speciation might have been the uplift events on the eastern QTP, although the timing of these events is controversial (Wang *et al.*, 2008; Deng and Ding, 2015; Renner, 2016; Su *et al.*, 2019). The QTP has experienced phased uplifts since the Eocene (Wang *et al.*, 2014; Favre *et al.*,

2015), but these events were heterogeneous both spatially and temporally. Indeed, different parts of the QTP have different uplift histories as well as climatic histories (Mulch and Chamberlain, 2006; Deng and Ding, 2015; Favre *et al.*, 2015; Muellner-Riehl, 2019). By the late Pliocene, mountain uplifts on the eastern QTP (including the Hengduan Mountains, HDM) were completed (~3.6 Mya; Sun *et al.*, 2011; Xing and Ree, 2017), and vegetation reconstruction based on macrofossil floras suggested that the southeastern QTP had likely reached roughly its current elevation by around the same period (Sun *et al.*, 2011). The rugged terrain of the HDM may have acted as a natural geographical barrier to pollen flow and seed dispersal for many taxa in this region (Feng *et al.*, 2016; Shahzad *et al.*, 2017; Ru *et al.*, 2018; Zhang *et al.*, 2018; Li *et al.*, 2020*b*). The *fastsimcoal2* analysis suggested that the common ancestor of *J. microsperma* and *J. erectopatens* experienced a population expansion about 4.52 Mya (Fig. 5B). The geological changes during the late Pliocene with the uplift of the HDM might have fragmented these populations which ultimately diverged under the influence of genetic drift and adapted to different habitats giving rise to the lineages of *J. microsperma* and *J. erectopatens*. The divergence of several conifer lineages which are endemic to the QTP and the HDM have also been associated with the uplift of the HDM in the late Pliocene (Sun et al., 2018, Ma et al., 2019, Li et al., 2020).

Adaptation to different habitats of the two junipers

Elucidating the genetic basis of local adaptation to environmental factors is crucial for the understanding of plant evolution. In the long term, local adaptation helps plants to face selection pressures due to climate change and environmental heterogeneity. We found genetic evidence that *J. microsperma* and *J. erectopatens* may have adapted to different environmental stressors. A total of 183 and 85 loci were identified as positively selected candidate genes in *J. microsperma* and *J.*

559 *erectopatens*, respectively, however, only in *J. microsperma* significant GO enrichment categories
560 were detected (Supplementary Data Tables S6 and S7). Enriched categories included response to
561 decreased oxygen levels, aerenchyma formation and response to external stimulus (Supplementary
562 Data Table S6). Aerenchyma is a cavity-filled parenchymatous tissue which can be found in the
563 roots, stems and leaves, especially from plants growing in oxygen deficient environments
564 (Schussler and Longstreth, 1996; Watkin *et al.*, 1998). The presence of *J. microsperma* at high
565 altitudes (3150-3350 m) which are characterized by lower oxygen levels and stronger UV radiation
566 compared to lower altitudes, might have contributed to the positive selection of the related genes
567 to adapt to these environmental stressors. Furthermore, genes related to the regulation of the
568 salicylic acid biosynthetic process, the positive regulation of the salicylic acid mediated signaling
569 pathway, and the response to trehalose were also enriched (Supplementary Data Table S6).
570 Salicylic acid, a phenolic compound, and trehalose, a disaccharide, play a role in the resistance of
571 plants to stress (Ding *et al.*, 2002; Kaplan *et al.*, 2004). These positively selected genes about stress
572 resistance might have resulted from the climate oscillation and constant environmental changes
573 occurred during the evolutionary history of *J. microsperma*.

574 Although no significant GO enrichment categories were detected in *J. erectopatens*, four GO
575 enrichment including the glycosyl and organonitrogen compound biosynthetic process as well as
576 the antiporter and secondary active transmembrane transporter activity were close to being
577 significant ($0.07 < P < 0.08$; Supplementary Data Table S7). The GO enrichment categories found
578 in *J. erectopatens* are not overlapping with those detected in *J. microsperma*, which suggests that
579 the evolution of the species pair may have responded to different environmental stressors.

580 Furthermore, our results suggest that based on the local climate data for the period between 1970
581 and 2000, thousands of SNPs are associated with the climate variables BIO3, BIO10, BIO17 and

582 BIO19, out of which 2,127 SNPs were shared between all four variables. In addition, we identified
583 49 categories of genes associated with the local environment (Table S8). Six of these gene
584 categories are involved in the response to abiotic and biotic stimuli, such as the immune system
585 process, the ethylene biosynthetic process, the response to oxygen-containing compounds, the
586 defense of insects, the response to stress, and the response to hormones (Table 3). Also, we found
587 several gene categories related to habitat adaptation, such as the carbohydrate metabolic process,
588 embryo development, and reproduction (Table S8). There was also an overlap between
589 significantly enriched gene categories of positively selected genes and climate-associated SNPs
590 (Tables S6, S8). This indicates that the two studied juniper species have the capacity to adapt to
591 climatic and environmental fluctuations, suggesting that this ability might have been an important
592 factor in their survival and the adaptation to historical abiotic and biotic stressors.
593
594 ***Conservation implications***
595 Narrow endemics such as *J. microsperma* and *J. erectopatens* are very vulnerable to extinction,
596 especially in a rapidly changing climate and during increased habitat fragmentation. However,
597 many of the remaining trees in fragmented populations may serve as reproductively viable
598 individuals and would therefore be very important for the long-term recovery of populations and
599 genetic conservation programs (Ralls, Sunnucks, Lacy, & Frankham, 2020). Thus, studying the
600 genetic diversity and demographic history of threatened species may inform conservation
601 programs of these species.
602 Based on our field surveys of recent years, it is likely that the two studied juniper species
603 would be evaluated as “Endangered” according to IUCN Red List criteria (IUCN, 2012) (see also
604 Shang *et al.*, 2015; Tso *et al.*, 2019; Xu *et al.*, 2019). Therefore, conservation measures should be

taken to minimize the risk of extinction. Based on the relatively low genetic diversity and high θ_π(0-fold)/θ_π(4-fold) ratio of *J. microsperma* compared to *J. erectopatens*, this species is likely to have a higher genetic load than *J. erectopatens*. This suggests lower fitness at the population level which might increase the probability of extinction (Klekowski, 1988; Glémin *et al.*, 2003; Stewart *et al.*, 2017). Moreover, our field surveys from 2011 to 2018 indicated that the area of occupancy and habitat quality of this rare juniper is declining due to human activities (Shang *et al.*, 2015; Tso *et al.*, 2019). It is therefore important to raise awareness in the local community of the importance of protecting *J. microsperma*.

Although *J. erectopatens* has higher genetic diversity and probably a lower genetic load than *J. microsperma*, only about 100 mature individuals occur in an area of around 2 km^2 at Anhong, Songpan, Sichuan (Xu *et al.*, 2019). No natural regeneration of *J. erectopatens* was evident during our field surveys, which might indicate that this species has a higher risk of extinction compared to *J. microsperma*. In this case, seed collection for *ex-situ* conservation and artificial breeding programs using seeds and cuttings should be considered as top priority conservation actions. Educating the local community on the ecological importance of *J. erectopatens* is an equally important measure to maintain and improve the long-term chances of its survival.

CONCLUSION

Here we presented the evidence that the uplifting of the eastern QTP triggered the speciation of two well-differentiated, narrow endemic juniper species, and that climatic changes in the last million years have shaped their demographic histories differently. Our study highlights the importance of speciation and demographic history reconstruction to understand the current

627 distribution pattern and genetic diversity level of threatened species and help to implement
628 conservation and management strategies.
629
630 **ACKNOWLEDGEMENTS**
631 This work was supported by the National Natural Science Foundation of China (grant numbers
632 31622015, 31590821), the National Basic Research Program of China (grant number
633 2014CB954100) and Sichuan University (Fundamental Research Funds for the Central
634 Universities, SCU2019D013, SCU2020D003). The Royal Botanic Garden Edinburgh is supported
635 by the Scottish Government's Rural and Environment Science and Analytical Services Division.
636
637 **AUTHOR CONTRIBUTIONS**
638 K.M. designed and supervised this study. J.M., W.W., J.L., J.X. managed fieldwork and collected
639 the materials. J.M., J.L. and H.Y. analyzed the data. J.M. and K.M. wrote the manuscript. P.F.,
640 R.M., M.R., G.M., L.O. revised the manuscript. J.M., P.F., W.W., M.R., H.Y. and K.M. finalized
641 the manuscript.
642
643 **LITERATURE CITED**
644 **Adams RP. 2014**. *Junipers of the world: the genus* Juniperus, 4th edn. Bloomington: Trafford Publishing.
645 **Adams RP, Schwarzbach AE. 2013**. Phylogeny of *Juniperus* using nrDNA and four cpDNA regions.
646 *Phytologia* **95**: 179–187.
647 **Akaike H. 1974**. A new look at the statistical model identification. *IEEE transactions on automatic control*
648 **19**: 716–723.
649 **Alexander DH, Lange K. 2011**. Enhancements to the ADMIXTURE algorithm for individual ancestry
650 estimation. *BMC Bioinformatics* **12**: 246.

Allendorf FW, Hohenlohe PA, Luikart G. 2010. Genomics and the future of conservation genetics. *Nature Reviews Genetics* **11**: 697–709.

Altschul SF, Madden TL, Schäffer AA, *et al*. 1997. Gapped BLAST and PSI-BLAST: a new generation of protein database search programs. *Nucleic Acids Research* **25**: 3389–3402.

Ashburner M, Ball CA, Blake JA, *et al*. 2000. Gene ontology: tool for the unification of biology. *Nature Genetics* **25**: 25–29.

Bairoch A, Apweiler R. 2000. The SWISS-PROT protein sequence database and its supplement TrEMBL in 2000. *Nucleic Acids Research* **28**: 45–48.

Barnosky AD, Matzke N, Tomiya S, *et al.* 2011. Has the Earth's sixth mass extinction already arrived? *Nature* **471**: 51–57.

Bolger AM, Lohse M, Usadel B. 2014. Trimmomatic: a flexible trimmer for Illumina sequence data. *Bioinformatics* **30**: 2114–2120.

Browning BL, Browning SR. 2013. Improving the accuracy and efficiency of identity-by-descent detection in population data. *Genetics* **194**: 459–471.

Casas-Marce M, Soriano L, López-Bao JV, Godoy JA. 2013. Genetics at the verge of extinction: insights from the Iberian lynx. *Molecular ecology* **22**: 5503–5515.

Ceballos G, Ehrlich PR, Barnosky AD, García A, Pringle RM, Palmer TM. 2015. Accelerated modern human-induced species losses: Entering the sixth mass extinction. *Science Advances* **1**: e1400253.

Ceballos G, Ehrlich PR, Dirzo R. 2017. Biological annihilation via the ongoing sixth mass extinction signaled by vertebrate population losses and declines. *Proceedings of the National Academy of Sciences* **114**: E6089–E6096.

Chen J-h, Huang Y, Brachi B, *et al*. 2019. Genome-wide analysis of Cushion willow provides insights into alpine plant divergence in a biodiversity hotspot. *Nature Communications* **10**: 5230.

Chen C, Chen H, Zhang Y, Thomas HR, Xia R. 2020. TBtools - an integrative toolkit developed for interactive analyses of big biological data. *Molecular Plant* **13**: 1194–1202.

Clark PU, Dyke AS, Shakun JD, *et al*. 2009. The last glacial maximum. *Science* **325**: 710–714.

Cronk Q. 2016. Plant extinctions take time. *Science* **353**: 446–447.

Danecek P, Auton A, Abecasis G, *et al*. 2011. The variant call format and VCFtools. *Bioinformatics* **27**: 2156–2158.

Deng T, Ding L. 2015. Paleoaltimetry reconstructions of the Tibetan Plateau: progress and contradictions. *National Science Review* **2**: 417–437.

DePristo MA, Banks E, Poplin R, *et al*. 2011. A framework for variation discovery and genotyping using next-generation DNA sequencing data. *Nature Genetics* **43**: 491–498.

Diffenbaugh NS, Giorgi F. 2012. Climate change hotspots in the CMIP5 global climate model ensemble. *Climatic Change* **114**: 813–822.

Ding C-K, Wang C, Gross KC, Smith DL. 2002. Jasmonate and salicylate induce the expression of pathogenesis-related-protein genes and increase resistance to chilling injury in tomato fruit. *Planta* **214**: 895–901.

Dirzo R, Young HS, Galetti M, Ceballos G, Isaac NJ, Collen B. 2014. Defaunation in the Anthropocene. *Science* **345**: 401–406.

Duan Y-W, Liu J-Q. 2006. Pollinator shift and reproductive performance of the Qinghai-Tibetan Plateau endemic and endangered *Swertia przewalskii* (Gentianaceae). *Biodiversity and Conservation* **16**: 1839–1850.

Ellegren H. 2014. Genome sequencing and population genomics in non-model organisms. *Trends in Ecology and Evolution* **29**: 51–63.

Ellegren H, Galtier N. 2016. Determinants of genetic diversity. *Nature Reviews Genetics* **17**: 422–433.

Excoffier L, Dupanloup I, Huerta-Sánchez E, Sousa VC, Foll M. 2013. Robust demographic inference from genomic and SNP data. *PLoS Genetics* **9**: e1003905.

Fan L, Zheng H, Milne RI, Zhang L, Mao K. 2018. Strong population bottleneck and repeated demographic expansions of *Populus adenopoda* (Salicaceae) in subtropical China. *Annals of Botany* **121**: 665–679.

Favre A, Päckert M, Pauls SU, *et al*. 2015. The role of the uplift of the Qinghai-Tibetan Plateau for the evolution of Tibetan biotas. *Biological Reviews* **90**: 236–253.

Feng L, Zheng Q-J, Qian Z-Q, *et al*. 2016. Genetic structure and evolutionary history of three alpine sclerophyllous oaks in east Himalaya-Hengduan Mountains and adjacent regions. *Frontiers in Plant Science* **7**: 1688.

Feng L, Ruhsam M, Wang YH, Li ZH, Wang XM. 2020. Using demographic model selection to untangle allopatric divergence and diversification mechanisms in the *Rheum palmatum* complex in the Eastern Asiatic Region. *Molecular Ecology* **29**: 1791–1805

Fjeldså J. 1994. Geographical patterns for relict and young species of birds in Africa and South America and implications for conservation priorities. *Biodiversity and Conservation* **3**: 207–226.

Foote AD, Vijay N, Ávila-Arcos MC, *et al*. 2016. Genome-culture coevolution promotes rapid divergence of killer whale ecotypes. *Nature Communications* **7**: 11693.

Frankham R. 1997. Do island populations have less genetic variation than mainland populations? *Heredity* **78**: 311–327.

Frankham R, Lees K, Montgomery ME, England PR, Lowe EH, Briscoe DA. 1999. Do population size bottlenecks reduce evolutionary potential? *Animal Conservation* **2**: 255–260.

Frankham R. 2005. Genetics and Extinction. *Biological Conservation* **126**: 131–140.

Freeland JR. 2020. *Molecular Ecology.* Oxford: John Wiley & Sons Ltd.

Frichot E, François O. 2015. LEA: An R package for landscape and ecological association studies. *Methods in Ecology and Evolution* **6**: 925–929.

Frichot E, Schoville SD, Bouchard G, François O. 2013. Testing for associations between loci and environmental gradients using latent factor mixed models. *Molecular Biology and Evolution* **30**: 1687–1699.

Fu Y, Li S, Guo Q, Zheng W, Yang R, Li H. 2019. Genetic diversity and population structure of two endemic *Cupressus* (Cupressaceae) species on the Qinghai-Tibetan plateau. *Journal of Genetics* **98**: 14.

Fu P-C, Sun S-S, Khan G, *et al*. 2020. Population subdivision and hybridization in a species complex of *Gentiana* in the Qinghai-Tibetan Plateau. *Annals of Botany* **125**: 677–690.

Fuentes-Pardo AP, Ruzzante DE. 2017. Whole-genome sequencing approaches for conservation biology: Advantages, limitations and practical recommendations. *Molecular Ecology* **26**: 5369–5406.

Garner BA, Hand BK, Amish SJ, *et al*. 2016. Genomics in conservation: case studies and bridging the gap between data and application. *Trends in Ecology and Evolution* **31**: 81–83.

Glémin S. 2003. How are deleterious mutations purged? Drift versus nonrandom mating. *Evolution* **57**, 2678–2687.

Goodwin S, McPherson JD, McCombie WR. 2016. Coming of age: ten years of next-generation sequencing technologies. *Nature Reviews Genetics* **17**: 333–351.

Grabherr MG, Haas BJ, Yassour M, *et al*. 2011. Full-length transcriptome assembly from RNA-Seq data without a reference genome. *Nature Biotechnology* **29**: 644–652.

Hahn MW. 2019. *Molecular Population Genetics*. New York: Sinauer Associates.

Hamabata T, Kinoshita G, Kurita K, *et al*. 2019. Endangered island endemic plants have vulnerable genomes. *Communications Biology* **2**: 244.

Hansen CCR, Hvilsom C, Schmidt NM, *et al*. 2018. The muskox lost a substantial part of its genetic diversity on its long road to Greenland. *Current Biology* **28**: 4022–4028. e5.

Harrisson KA, Pavlova A, Telonis-Scott M, Sunnucks P. 2014. Using genomics to characterize evolutionary potential for conservation of wild populations. *Evolutionary Applications* **7**: 1008–1025.

He Y, Lu A, Zhang Z, Pang H, Zhao J. 2005. Seasonal variation in the regional structure of warming across China in the past half century. *Climate Research* **28**: 213–219.

Hijmans RJ, Cameron SE, Parra JL, Jones PG, Jarvis A. 2005. Very high resolution interpolated climate surfaces for global land areas. *International Journal of Climatology: A Journal of the Royal Meteorological Society* **25**: 1965–1978.

Hijmans RJ, Phillips S, Leathwick J, Elith J. 2015. R package dismo: species distribution modeling, version 1.0-12.(Available online at: http://cran.r-project.org/web/packages/dismo/index.html)

Hou J, D'Andrea WJ, Wang M, He Y, Liang J. 2017. Influence of the Indian monsoon and the subtropical jet on climate change on the Tibetan Plateau since the late Pleistocene. *Quaternary Science Reviews* **163**: 84–94.

Huang J, Yang L-Q, Yu Y, *et al.* 2018. Molecular phylogenetics and historical biogeography of the tribe Lilieae (Liliaceae): bi-directional dispersal between biodiversity hotspots in Eurasia. *Annals of Botany* **122**: 1245–1262.

Hudson RR, Kreitman M, Aguadé M. 1987. A test of neutral molecular evolution based on nucleotide data. *Genetics* **116**: 153–159.

Hung C-M, Shaner P-JL, Zink RM, *et al.* 2014. Drastic population fluctuations explain the rapid extinction of the passenger pigeon. *Proceedings of the National Academy of Sciences* **111**: 10636–10641.

IUCN. 2012. *IUCN Red List Categories and Criteria: Version 3.1*. Gland, Switzerland and Cambridge, UK: IUCN.

Jacquemyn H, Vandepitte K, Roldán-Ruiz I, Honnay O. 2009. Rapid loss of genetic variation in a founding population of *Primula elatior* (Primulaceae) after colonization. *Annals of Botany* **103**: 777–783.

Kaplan F, Kopka J, Haskell DW, *et al.* 2004. Exploring the temperature-stress metabolome of *Arabidopsis*. *Plant Physiology* **136**: 4159–4168.

Keller LF, Waller DM. 2002. Inbreeding effects in wild populations. *Trends in Ecology and Evolution* **17**: 230–241.

Klekowski EJ. 1988. Genetic load and its causes in long-lived plants. *Trees-Structure and Function* **2**: 195–203.

López-Pujol J, Zhang FM, Sun HQ, Ying TS, Ge S. 2011. Centres of plant endemism in China: places for survival or for speciation? *Journal of Biogeography* **38**: 1267–1280.

Li W, Godzik A. 2006. Cd-hit: a fast program for clustering and comparing large sets of protein or nucleotide sequences. *Bioinformatics* **22**: 1658–1659.

Li H, Durbin R. 2009. Fast and accurate short read alignment with Burrows-Wheeler transform. *Bioinformatics* **25**: 1754–1760.

Li H, Handsaker B, Wysoker A, *et al*. 2009. The sequence alignment/map format and SAMtools. *Bioinformatics* **25**: 2078–2079.

Li Z, Zou J, Mao K, *et al*. 2012. Population genetic evidence for complex evolutionary histories of four high altitude juniper species in the Qinghai-Tibetan Plateau. *Evolution* **66**: 831–845.

Li F, Markus R, Wang Y-H, Li Z-H, Wang X-M. 2020*a*. Using demographic model selection to untangle allopatric divergence and diversification mechanisms in the *Rheum palmatum* complex in the Eastern Asiatic Region. *Molecular Ecology* **29**: 1791–1805.

Li J, Milne RI, Ru D, *et al*. 2020*b*. Allopatric divergence and hybridization within *Cupressus chengiana* (Cupressaceae), a threatened conifer in the northern Hengduan Mountains of western China. *Molecular Ecology* **29**: 1250–1266.

Lima JS, Telles MP, Chaves LJ, Lima-Ribeiro MS, Collevatti RG. 2017. Demographic stability and high historical connectivity explain the diversity of a savanna tree species in the Quaternary. *Annals of Botany* **119**: 645–657.

Liu X-L, Qian Z-G, Liu F-H, Yang Y-W, Pu C-X. 2011. Genetic diversity within and among populations of *Neopicrorhiza scrophulariiflora* (Scrophulariaceae) in China, an endangered medicinal plant. *Biochemical Systematics and Ecology* **39**: 297–301.

Liu J, Moeller M, Provan J, Gao LM, Poudel RC, Li DZ. 2013. Geological and ecological factors drive cryptic speciation of yews in a biodiversity hotspot. *New Phytologist* **199**: 1093–1108.

Liu JQ, Duan YW, Hao G, Ge XJ, Sun H. 2014. Evolutionary history and underlying adaptation of alpine plants on the Qinghai-Tibet Plateau. *Journal of Systematics and Evolution* **52**: 241–249.

Liu X, Fu Y-X. 2015. Exploring population size changes using SNP frequency spectra. *Nature Genetics* **47**: 555–559.

Ma Y, Wang J, Hu Q, *et al.* 2019. Ancient introgression drives adaptation to cooler and drier mountain habitats in a cypress species complex. *Communications Biology* **2**: 213.

Mao K, Ruhsam M, Ma Y, *et al.* 2019. A transcriptome-based resolution for a key taxonomic controversy in Cupressaceae. *Annals of Botany* **123**: 153–167.

Marsden CD, Ortega-Del Vecchyo D, O'Brien DP *et al.* 2016. Bottlenecks and selective sweeps during domestication have increased deleterious genetic variation in dogs. *Proceedings of the National Academy of Sciences* **113**:152–157.

Miraldo A, Li S, Borregaard MK, *et al.* 2016. An Anthropocene map of genetic diversity. *Science* **353**: 1532–1535.

Mosbrugger V, Favre A, Muellner-Riehl AN, Päckert M, Mulch A. 2018. *Cenozoic evolution of geo-biodiversity in the Tibeto-Himalayan region. Mountains, Climate, and Biodiversity*. Hoboken: John Wiley & Sons.

Muellner-Riehl AN. 2019. Mountains as evolutionary arenas: patterns, emerging approaches, paradigm shifts, and their implications for plant phylogeographic research in the Tibeto-Himalayan Region. *Frontiers in Plant Science* **10**: 195.

Mulch A, Chamberlain CP. 2006. The rise and growth of Tibet. *Nature* **439**: 670–671.

Nei M, Li W-H. 1979. Mathematical model for studying genetic variation in terms of restriction endonucleases. *Proceedings of the National Academy of Sciences* **76**: 5269–5273.

Nevado B, Contreras-Ortiz N, Hughes C, Filatov DA. 2018. Pleistocene glacial cycles drive isolation, gene flow and speciation in the hig-elevation Andes. *New Phytologist* **219**: 779–793.

O'Brien SJ. 1994. A role for molecular genetics in biological conservation. *Proceedings of the National Academy of Sciences* **91**: 5748–5755.

827 **Ouborg NJ, Pertoldi C, Loeschcke V, Bijlsma RK, Hedrick PW. 2010**. Conservation genetics in
828 transition to conservation genomics. *Trends in Genetics* **26**: 177–187.

829 **Owen LA, Dortch JM. 2014**. Nature and timing of Quaternary glaciation in the Himalayan-Tibetan
830 orogen. *Quaternary Science Reviews* **88**: 14–54.

831 **Pautasso M. 2009**. Geographical genetics and the conservation of forest trees. *Perspectives in Plant*
832 *Ecology, Evolution and Systematics* **11**: 157–189.

833 **Petit RJ, Hu FS, & Dick CW. 2008.** Forests of the past: a window to future changes. *Science* **320**:1450–
834 1452.

835 **Price AL, Patterson NJ, Plenge RM, Weinblatt ME, Shadick NA, Reich D. 2006**. Principal
836 components analysis corrects for stratification in genome-wide association studies. *Nature*
837 *Genetics* **38**: 904–909.

838 **Purcell S, Neale B, Todd-Brown K, *et al*. 2007**. PLINK: a tool set for whole-genome association and
839 population-based linkage analyses. *The American Journal of Human Genetics* **81**: 559–575.

840 **Rahbek C, Borregaard MK, Antonelli A, *et al*. 2019**. Building mountain biodiversity: Geological and
841 evolutionary processes. *Science* **365**: 1114–1119.

842 **Ralls K, Sunnucks P, Lacy RC, & Frankham R. 2020**. Genetic rescue: a critique of the evidence supports
843 maximizing genetic diversity rather than minimizing the introduction of putatively harmful genetic
844 variation. *Biological Conservation* **251**: 108784.

845 **Ren G, Mateo RG, Liu J, *et al*. 2017**. Genetic consequences of Quaternary climatic oscillations in the
846 Himalayas: *Primula tibetica* as a case study based on restriction site-associated DNA sequencing.
847 *New Phytologist* **213**: 1500–1512.

848 **Renner SS. 2016**. Available data point to a 4-km-high Tibetan Plateau by 40 Ma, but 100 molecular-clock
849 papers have linked supposed recent uplift to young node ages. *Journal of Biogeography* **43**: 1479–
850 1487.

Rogers RL, Slatkin M. 2017. Excess of genomic defects in a woolly mammoth on Wrangel island. *PLoS Genetics* **13**: e1006601.

Ru D, Mao K, Zhang L, Wang X, Lu Z, Sun Y. 2016. Genomic evidence for polyphyletic origins and interlineage gene flow within complex taxa: a case study of *Picea brachytyla* in the Qinghai-Tibet Plateau. *Molecular Ecology* **25**: 2373–2386.

Ru D, Sun Y, Wang D, *et al*. 2018. Population genomic analysis reveals that homoploid hybrid speciation can be a lengthy process. *Molecular Ecology* **27**: 4875–4887.

Saccheri I, Kuussaari M, Kankare M, Vikman P, Fortelius W, Hanski I. 1998. Inbreeding and extinction in a butterfly metapopulation. *Nature* **392**: 491–494.

Schussler EE, Longstreth DJ. 1996. Aerenchyma develops by cell lysis in roots and cell separation in leaf petioles in *Sagittaria lancifolia* (Alismataceae). *American Journal of Botany* **83**: 1266–1273.

Segelbacher G, Cushman SA, Epperson BK, *et al*. 2010. Applications of landscape genetics in conservation biology: concepts and challenges. *Conservation Genetics* **11**: 375–385.

Shahzad K, Jia Y, Chen F-L, Zeb U, Li Z-H. 2017. Effects of mountain uplift and climatic oscillations on phylogeography and species divergence in four endangered *Notopterygium* herbs. *Frontiers in Plant Science* **8**: 1929.

Shang H-Y, Li Z-H, Dong M, Adams R, Miehe G, Opgenoorth L, Mao K-S. 2015. Evolutionary origin and demographic history of an ancient conifer (*Juniperus microsperma*) in the Qinghai-Tibetan Plateau. *Scientific Reports* **5**: 10216.

Shimono A, Ueno S, Gu S, Zhao X, Tsumura Y, Tang Y. 2010. Range shifts of *Potentilla fruticosa* on the Qinghai-Tibetan Plateau during glacial and interglacial periods revealed by chloroplast DNA sequence variation. *Heredity* **104**: 534–542.

Spielman D, Brook BW, Frankham R. 2004. Most species are not driven to extinction before genetic factors impact them. *Proceedings of the National Academy of Sciences* **101**: 15261–15264.

Spicer R, Su T, Valdes P, Farnsworth A, Wu F-X, Shi G, Spicer T, Zhou Z-K. 2021. Why 'the uplift of the Tibetan Plateau' is a myth? *National Science Review* : nwaa091

Stamatakis A. 2014. RAxML version 8: a tool for phylogenetic analysis and post-analysis of large phylogenies. *Bioinformatics* **30**: 1312–1313.

Stoffel M, Humble E, Paijmans A, *et al.* 2018. Demographic histories and genetic diversity across pinnipeds are shaped by human exploitation, ecology and life-history. *Nature Communications* **9**: 4836.

Stewart GS, Morris MR, Genis AB, Szűcs M, Melbourne BA, Tavener SJ, Hufbauer RA. 2017. The power of evolutionary rescue is constrained by genetic load. *Evolutionary Applications* **10**: 731–741.

Su T, Farnsworth A, Spicer R, *et al.* 2019. No high tibetan plateau until the neogene. *Science Advances* **5**: eaav2189.

Sun B-N, Wu J-Y, Liu Y-SC, *et al.* 2011. Reconstructing Neogene vegetation and climates to infer tectonic uplift in western Yunnan, China. *Palaeogeography, Palaeoclimatology, Palaeoecology* **304**: 328–336.

Sun Y, Abbott RJ, Li L, Li L, Zou J, Liu J. 2014. Evolutionary history of Purple cone spruce (*Picea purpurea*) in the Qinghai-Tibet Plateau: homoploid hybrid origin and Pleistocene expansion. *Molecular Ecology* **23**: 343–359.

Sun Y, Abbott RJ, Lu Z, *et al.* 2018. Reticulate evolution within a spruce (*Picea*) species complex revealed by population genomic analysis. *Evolution* **72**: 2669–2681.

Tajima F. 1989*a*. The effect of change in population size on DNA polymorphism. *Genetics* **123**: 597–601.

Tajima F. 1989*b*. Statistical method for testing the neutral mutation hypothesis by DNA polymorphism. *Genetics* **123**: 585–595.

Thompson Lo, Yao T, Davis M, *et al.* 1997. Tropical climate instability: The last glacial cycle from a Qinghai-Tibetan ice core. *Science* **276**: 1821–1825.

Todd EV, Black MA, Gemmell NJ. 2016. The power and promise of RNA-seq in ecology and evolution. *Molecular Ecology* **25**: 1224–1241.

902 **Tso S, Li J, Xie S, *et al.*** 2019. Characterization of the complete chloroplast genome of *Juniperus*
903 *microsperma* (Cupressaceae), a rare endemic from the Qinghai-Tibet Plateau. *Conservation*
904 *Genetics Resources* **11:** 325–328.
905 **Uchiyama I, Higuchi T, Kawai M. 2009**. MBGD update 2010: toward a comprehensive resource for
906 exploring microbial genome diversity. *Nucleic Acids Research* **38**: D361–D365.
907 **Wang Y–J, Liu J–Q, Miehe G. 2007**. Phylogenetic origins of the Himalayan endemic *Dolomiaea*,
908 *Diplazoptilon* and *Xanthopappus* (Asteraceae: Cardueae) based on three DNA regions. *Annals of*
909 *Botany* **99**: 311–322.
910 **Wang C, Zhao X, Liu Z, *et al*. 2008**. Constraints on the early uplift history of the Tibetan Plateau.
911 *Proceedings of the National Academy of Sciences* **105**: 4987–4992.
912 **Wang L, Abbott RJ, Zheng W *et al*. 2009**. History and evolution of alpine plants endemic to the Qinghai–
913 Tibetan Plateau: *Aconitum gymnandrum* (Ranunculaceae). *Molecular Ecology* **18**: 709–721.
914 **Wang C, Dai J, Zhao X, *et al*. 2014**. Outward–growth of the Tibetan Plateau during the Cenozoic: A
915 review. *Tectonophysics* **621**: 1–43.
916 **Wang A, Li W. 2016**. Genetic diversity of *Rheum tanguticum* (Polygonaceae), an endangered species on
917 Qinghai–Tibetan Plateau. *Biochemical Systematics and Ecology* **69**: 132–137.
918 **Wang P, Burley JT, Liu Y, *et al*. 2021**. Genomic Consequences of Long-Term Population Decline in
919 Brown Eared Pheasant. *Molecular Biology and Evolution* **38**:263–273.
920 **Wang X, Chai K, Liu S, Wei J, Jiang Z, Liu Q. 2017**. Changes of glaciers and glacial lakes implying
921 corridor–barrier effects and climate change in the Hengduan Shan, southeastern Tibetan Plateau.
922 *Journal of Glaciology* **63**: 535–542.
923 **Wang Y, Liang Q, Hao G, Chen C, Liu J. 2018**. Population genetic analyses of the endangered alpine
924 *Sinadoxa corydalifolia* (Adoxaceae) provide insights into future conservation. *Biodiversity and*
925 *Conservation* **27**: 2275–2291.

Watkin EL, Thomson CJ, Greenway H. 1998. Root development and aerenchyma formation in two wheat cultivars and one triticale cultivar grown in stagnant agar and aerated nutrient solution. *Annals of Botany* **81**: 349–354.

Watterson G. 1975. On the number of segregating sites in genetical models without recombination. *Theoretical Population Biology* **7**: 256–276.

Weir BS, Cockerham CC. 1984. Estimating F–statistics for the analysis of population structure. *Evolution* **38**: 1358–1370.

Wen J, Zhang J, Nie Z–L, Zhong Y, Sun H. 2014. Evolutionary diversifications of plants on the Qinghai–Tibetan Plateau. *Frontiers in Genetics* **5**: 4.

Xing Y, Ree RH. 2017. Uplift–driven diversification in the Hengduan Mountains, a temperate biodiversity hotspot. *Proceedings of the National Academy of Sciences* **114**: E3444–E3451.

Xu J, Song X, Ruhsam M, *et al*. 2019. Distinctiveness, speciation and demographic history of the rare endemic conifer *Juniperus erectopatens* in the eastern Qinghai–Tibet Plateau. *Conservation Genetics* **20**: 1289–1301.

Yang W, Yao T, Xu B, Ma L, Wang Z, Wan M. 2010. Characteristics of recent temperate glacier fluctuations in the Parlung Zangbo River basin, southeast Tibetan Plateau. *Chinese Science Bulletin* **55**: 2097–2102.

Yi X, Liang Y, Huerta–Sanchez E, *et al*. 2010. Sequencing of 50 human exomes reveals adaptation to high altitude. *Science* **329**: 75–78.

Yokoyama Y, Lambeck K, De Deckker P, Johnston P, Fifield LK. 2000. Timing of the Last Glacial Maximum from observed sea–level minima. *Nature* **406**: 713–716.

Yu Z, McAndrews JH, Eicher U. 1997. Middle Holocene dry climate caused by change in atmospheric circulation patterns: evidence from lake levels and stable isotopes. *Geology* **25**: 251–254.

Zhang DC, Ye JX, Sun H. 2016. Quantitative approaches to identify floristic units and centres of species endemism in the Qinghai–Tibetan Plateau, south–western China. *Journal of Biogeography* **43**: 2465–2476.

Zhang J–M, López–Pujol J, Gong X, Wang H–F, Vilatersana R, Zhou S–L. 2018. Population genetic dynamics of Himalayan–Hengduan tree peonies, *Paeonia* subsect. *Delavayanae*. *Molecular Phylogenetics and Evolution* **125**: 62–77.

Zhang D, Hao GQ, Guo XY, Hu QJ, Liu JQ. 2019. Genomic insight into "sky island" species diversification in a mountainous biodiversity hotspot. *Journal of Systematics and Evolution* **57**: 633–645.

Zheng B, Rutter N. 1998. On the problem of Quaternary glaciations, and the extent and patterns of Pleistocene ice cover in the Qinghai–Xizang (Tibet) Plateau. *Quaternary International* **45**: 109–122.

Zheng B, Xu Q, Shen Y. 2002. The relationship between climate change and Quaternary glacial cycles on the Qinghai–Tibetan Plateau: review and speculation. *Quaternary International* **97**: 93–101.

Zhou S, Wang J, Xu L, Wang X, Colgan PM, Mickelson DM. 2010. Glacial advances in southeastern Tibet during late Quaternary and their implications for climatic changes. *Quaternary International* **218**: 58–66.

Zhou S, Li J, Zhao J, Wang J, Zheng J. 2011. Quaternary glaciations: extent and chronology in China. *Developments in Quaternary Sciences*. Amsterdam: Elsevier.

TABLES

Table 1 Location details of the sampled populations of *Juniperus microsperma* and *J. erectopatens*.

ID	Species	n[a]	Location	Latitude	Longitude	Altitude (m)
1	*J. microsperma*	8	Bomi Xizang	N29°36.98′	E96°19.92′	3,325
2	*J. microsperma*	12	Bomi Xizang	N29°37.12′	E96°18.98′	3,253
3	*J. microsperma*	5	Bomi Xizang	N29°37.29′	E96°18.05′	3,221
4	*J. microsperma*	5	Bomi Xizang	N29°38.94′	E96°13.13′	3,171
5	*J. microsperma*	17	Bomi Xizang	N29°39.94′	E96°12.34′	3,167
6	*J. microsperma*	9	Bomi Xizang	N29°40.78′	E96°12.56′	3,202
7	*J. erectopatens*	28	Songpan Sichuan	N32°27.94′	E103°40.06′	2,714

[a] n indicates the number of samples.

977 **Table 2** Population genetic statistics of *J. microsperma* and *J. erectopatens*.

Population	θ_π[a]	θ_w[b]	H_o[c]	H_e[d]	Tajima's *D*	F_{ST}[e] *J.erectopatens*	d_{XY}[f] *J.erectopatens*
J. microsperma	0.00129	0.00099	0.19768	0.16934	0.68151	0.23363	0.31924
J. erectopatens	0.00222	0.00139	0.36917	0.28872	1.50340	-	-

978

979 [a] θ_π nucleotide diversity calculated by pairwise differences between sequences.

980 [b] θ_w nucleotide diversity calculated by numbers of segregating sites between sequences.

981 [c] H_o observed heterozygosity.

982 [d] H_e expected heterozygosity.

983 [e] F_{ST} pairwise genetic distance.

984 [f] d_{XY} mean pairwise sequence divergence.

985

986 **Table 3** GO enrichment of environment associated genes (LFMM) within *J. microsperma* and *J.*
987 *erectopatens*.

GO.ID	Term	Annotated	Significant	Expected	classicFisher
GO:0002376	immune system process	39	4	1.33	4.10E-06
GO:0009693	ethylene biosynthetic process	26	3	0.88	5.00E-05
GO:1901700	response to oxygen-containing compound	99	2	3.37	0.03501
GO:0002213	defense response to insect	14	1	0.48	0.03798
GO:0006950	response to stress	291	6	9.9	0.04289
GO:0009725	response to hormone	17	1	0.58	0.04593

988

FIGURE DESCRIPTIONS

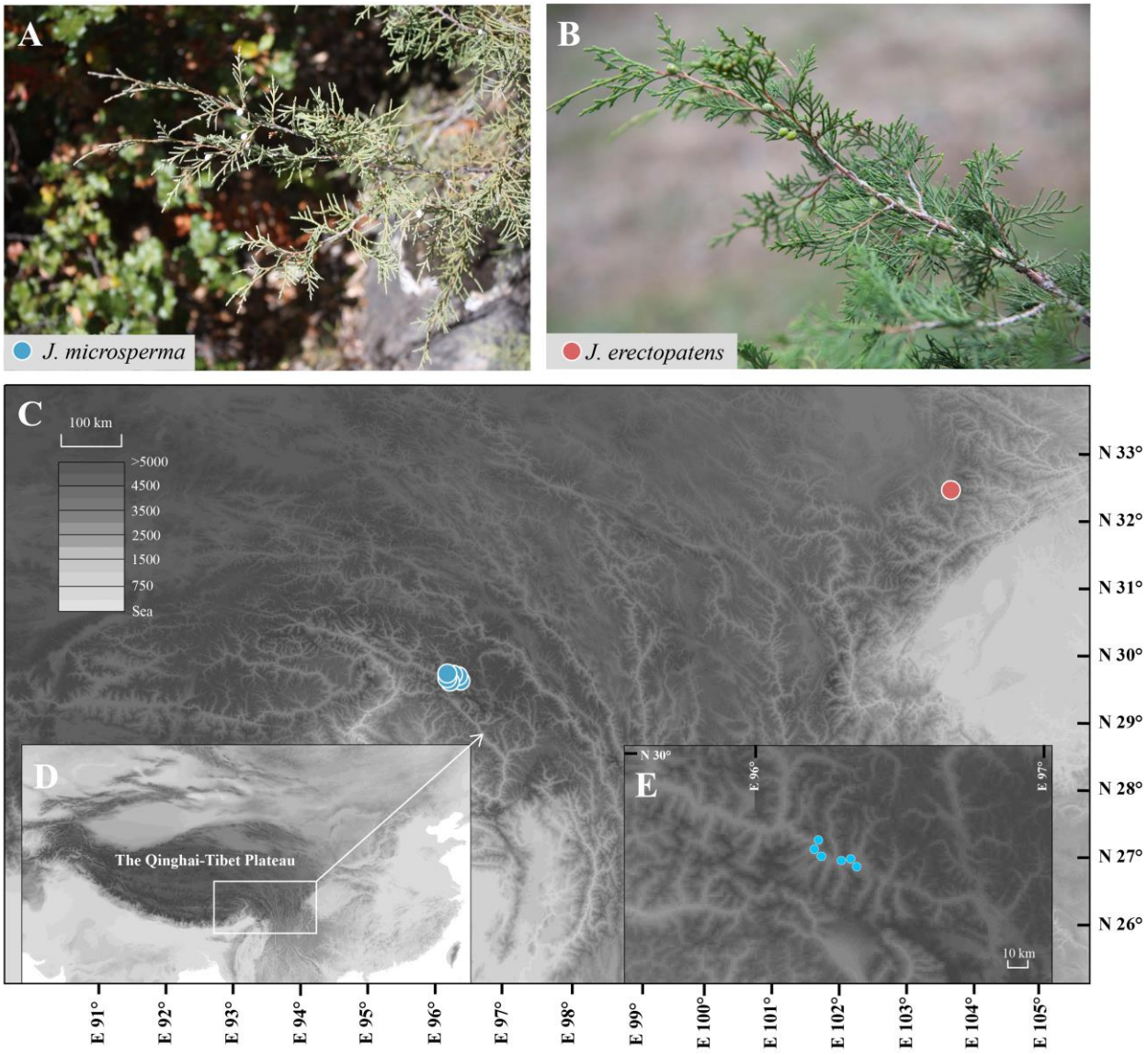

Figure 1. (A) Photo of *J. microsperma*. (B) Photo of *J. erectopatens*. (C) Location of sampled populations of *J. microsperma* and *J. erectopatens*. See also Table S1. (D) The location of the Qinghai-Tibet Plateau. (E) Sampling sites of *J. microsperma* along the Parlong Zangpo river.

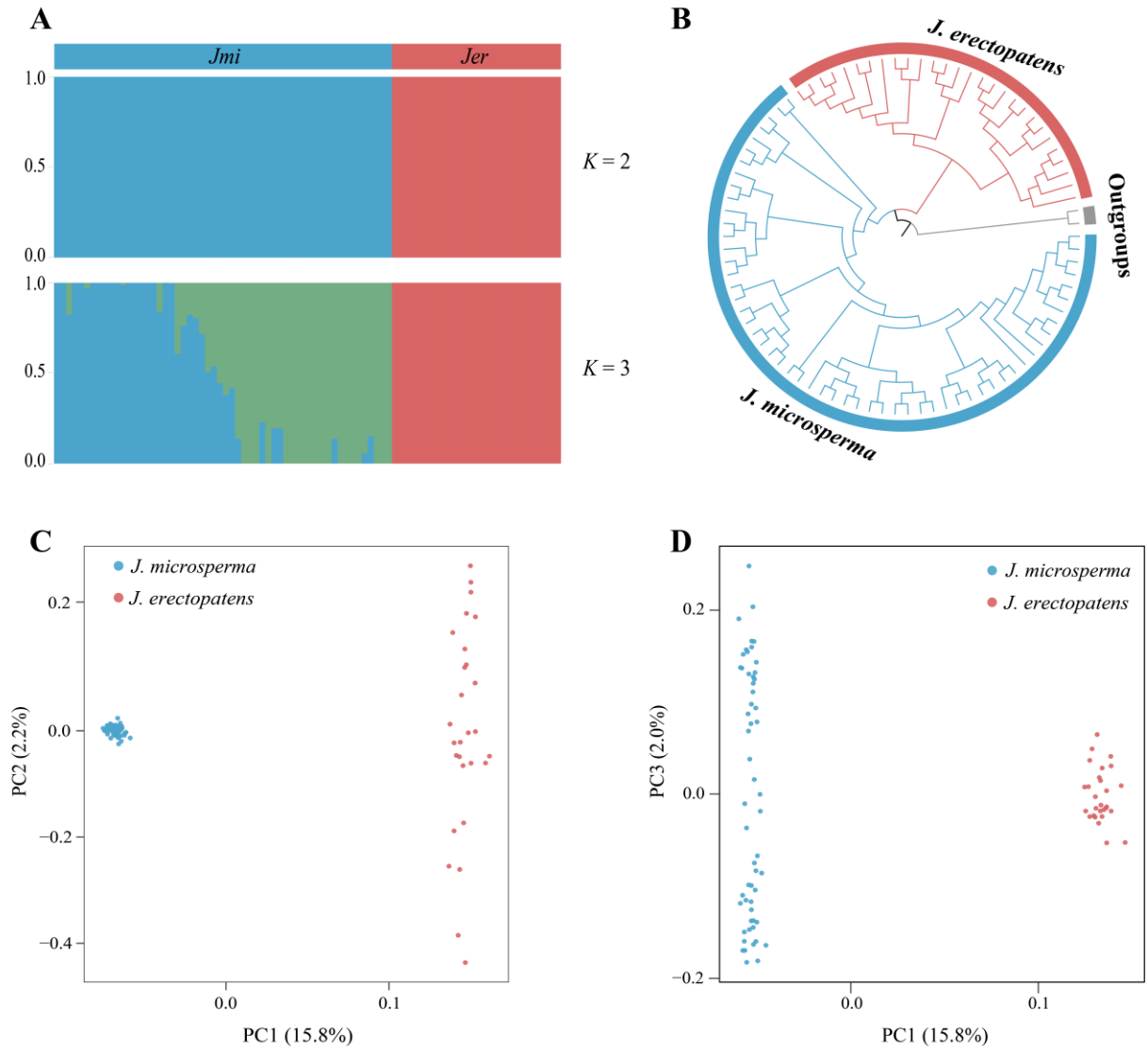

997

998 **Figure 2.** Population genetic and phylogenetic analyses of *J. microsperma* and *J. erectopatens*
999 based on 149,052 SNPs. (A) ADMIXTURE plots for K = 2 and 3. The *x*-axis shows the individuals
1000 of *J. microsperma* (*Jmi*) and *J. erectopatens* (*Jer*) with each vertical bar representative of an
1001 individual; the *y*-axis quantifies the proportion of an individual's inferred ancestry. See also
1002 Figures S2, S3. (B) Maximum likelihood phylogenetic tree. (C), (D) Principal component analysis
1003 (PCA) plots of the two studied species showing PC1 vs. PC2 and PC1 vs. PC3, respectively.

1004

1005

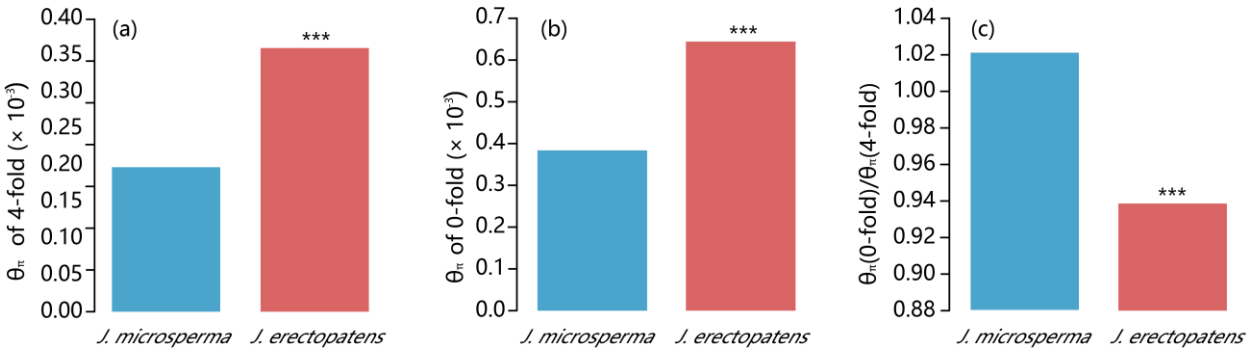

Figure 3. Population genetics statistics. (a)Nucleotide diversity (θ_π) on 4-fold degeneration sites. (b) Nucleotide diversity (θ_π) on 0-fold degeneration sites. (c) Nucleotide diversity (θ_π) of 0-fold degeneration sites over nucleotide diversity (θ_π) of 4-fold degeneration sites. For each statistic, *Juniperus erectopatens* populations were compared with the *J. microsperma* population. *** non-adjusted P<0.001.

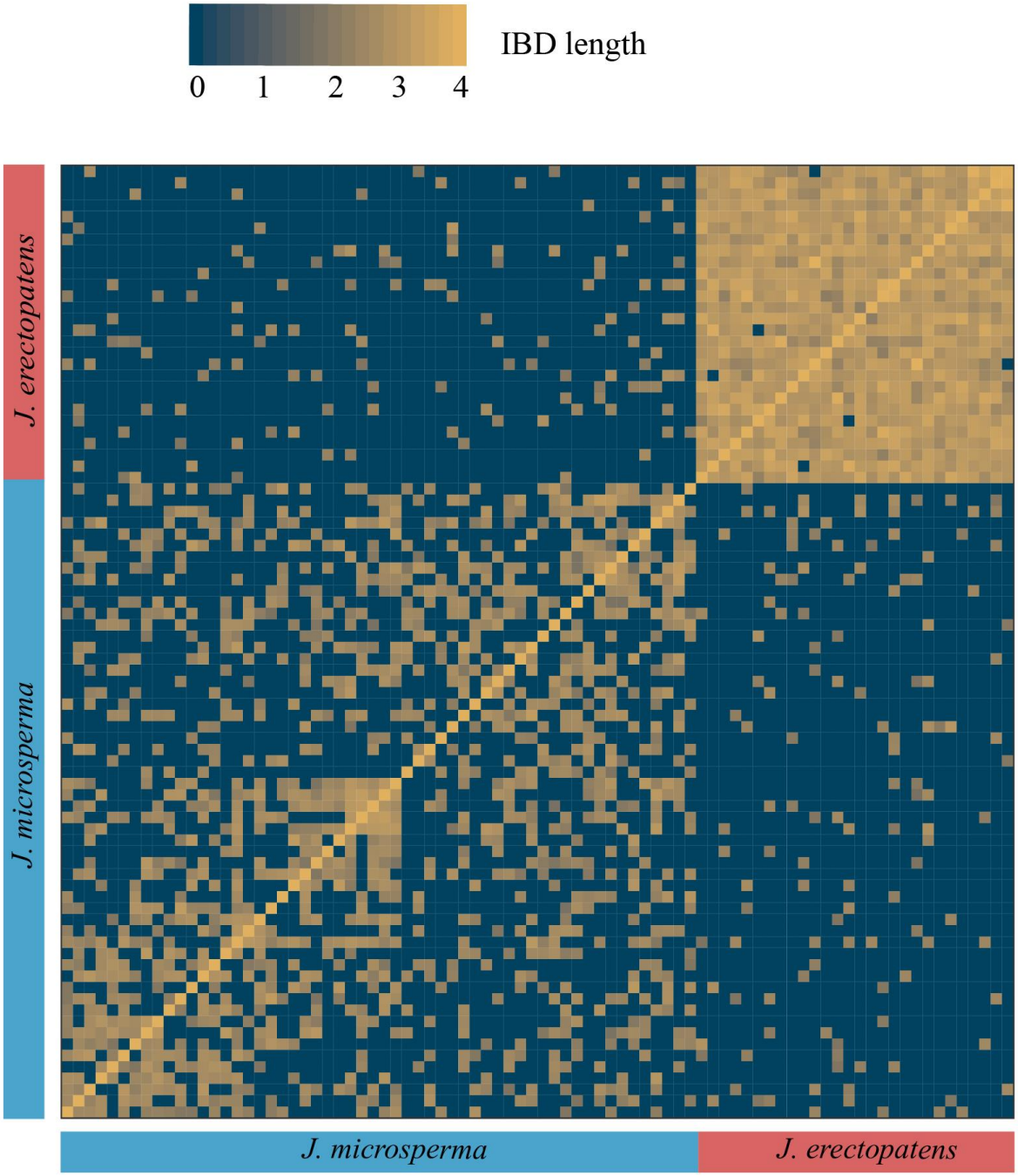

Figure 4. Estimation of shared haplotypes between individuals of *J. microsperma* and *J. erectopatens*. Heatmap colors represent the local length of IBD blocks for each pairwise comparison.

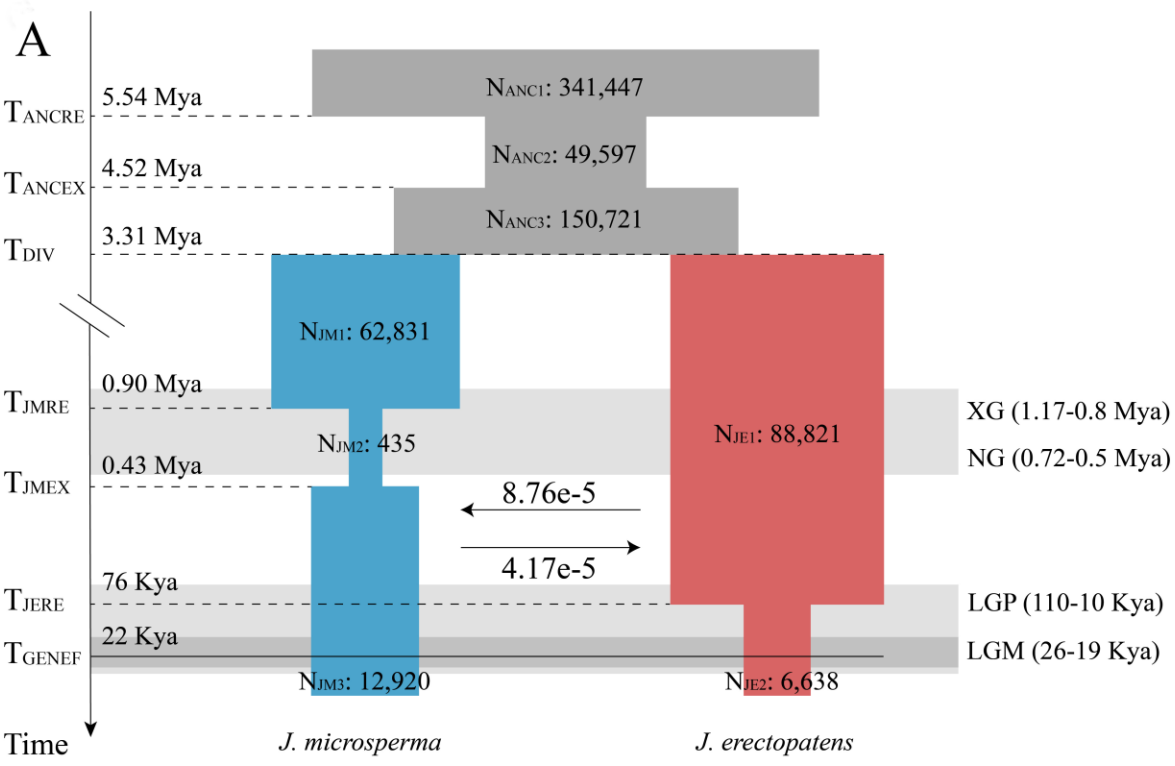
A
TANCRE
5.54 Mya
NANC1: 341,447
TANCEX
4.52 Mya
NANC2: 49,597
TDIV
3.31 Mya
NANC3: 150,721
NJM1: 62,831
TJMRE
0.90 Mya
NJM2: 435
NJE1: 88,821
XG (1.17-0.8 Mya)
NG (0.72-0.5 Mya)
TJMEX
0.43 Mya
8.76e-5
4.17e-5
TJERE
76 Kya
LGP (110-10 Kya)
TGENEF
22 Kya
LGM (26-19 Kya)
NJM3: 12,920
NJE2: 6,638
Time
J. microsperma
J. erectopatens

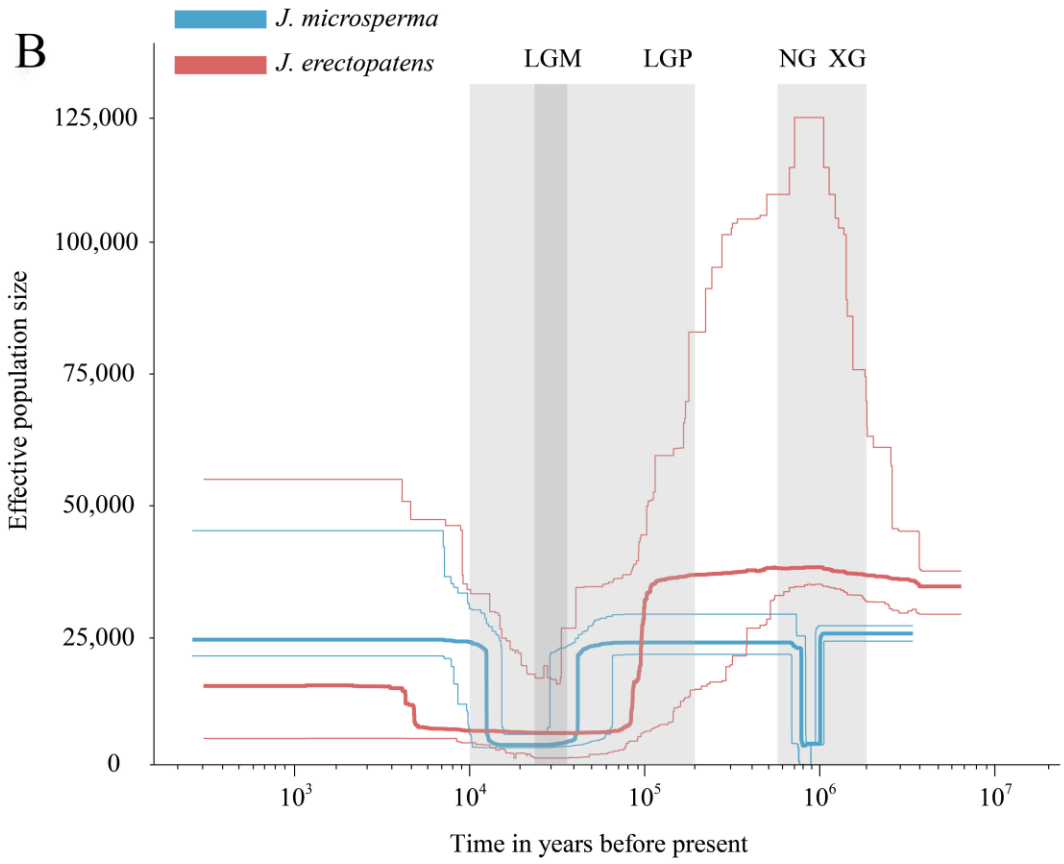
B
J. microsperma
J. erectopatens
LGM
LGP
NG XG
125,000
100,000
75,000
50,000
25,000
0
Effective population size
10^3
10^4
10^5
10^6
10^7
Time in years before present

1018

Figure 5. Demographic history of *J. microsperma* and *J. erectopatens*. The light gray areas represent different glaciation events during the Pleistocene (XG Xixiabangma Glaciation, NG Naynayxungla Glaciation, LGP Last Glaciation Period, LGM Last Glaciation Maximum). (A) Schematic illustration of the best demographic scenario using *fastsimcoal2*. Estimated effective population sizes (*N*), divergence time, bottleneck time and phased gene flow are indicated. The number next to the horizontal arrows represents the per generation migration rate between populations. The full line indicates the time when gene flow stopped. See also Table S4. (B) Changes in N_e over time in *J. microsperma* and *J. erectopatens* inferred by the Stairway Plot method. Thick and thin light lines represent the median and the 95% pseudo-CI defined by the 2.5% and 97.5% estimations, respectively, using the site frequency spectrum analysis.

SUPPORTING INFORMATION

Supplementary Table S1. Location information for sampled individual of *J. microsperma* and *J. erectopatens*.

Supplementary Table S2. Environmental variables used in this study.

Supplementary Table S3. Genetic diversity of *J. microsperma* and *J. erectopatens* populations based on seven randomly selected individuals per population apart from population 3 and 4 where only five individuals per population were available (Tables 1, S1).

Supplementary Table S4. Summary of parameters for the five final candidate models (Model-3-1 to Model-3-5) tested using *fastsimcoal2*. For each model, the table shows the maximum likelihood estimate (Likelihood), the number of parameters (No. of parameters), the Akaike's information criterion value (AIC), the difference in AIC value (Δ) and the value of AIC weight (w).

Supplementary Table S5. Inferred parameters and confidence intervals for the best-fitting demographic model presented in Figure 5A.

Supplementary Table S6. GO enrichment of positively selected genes (PSG) within *J. microsperma*. BP, Biological Process; MF, Molecular Function; CC, Cellular Component. The corrected *P*-value was employed to indicate the significance of enrichment. Underlined terms indicate shared terms between PSGs and climate associated SNPs.

Supplementary Table S7. GO enrichment of positively selected genes within *J. erectopatens*. BP, Biological Process; MF, Molecular Function; CC, Cellular Component. The corrected *P*-value was employed to indicate the significance of enrichment. Underlined terms indicate shared terms between PSGs and climate associated SNPs.

Supplementary Table S8. GO enrichment of environment associated genes (LFMM) within *J. microsperma* and *J. erectopatens*. Underlined terms indicate shared terms between PSGs and climate associated SNPs.

Supplementary Figure S1. Number of shared and species-specific SNPs in *J. microsperma* and *J. erectopatens*. The size of the circles is proportional to the number of SNPs. The overlap of the two circles represents the shared SNPs between species.

Supplementary Figure S2. The cross-validation (CV) error for each K value that was estimated using ADMIXTURE.

Supplementary Figure S3. Population structure plots for K=2 to K=4. The *x*-axis shows each individual of *J. microsperma* (*Jmi*) and *J. erectopatens* (*Jer*); the *y*-axis quantifies the proportion of an individual's inferred ancestry.

Supplementary Figure S4. Genetic differentiation between *J. microsperma* and *J. erectopatens*. (A) Distribution density of F_{ST} between *J. microsperma* and *J. erectopatens*. (B) Distribution density of d_{XY} between *J. microsperma* and *J. erectopatens*.

Supplementary Figure S5. Schematic illustration of candidate demographic models that were simulated and tested in *fastsimcoal2*, the value below every model is AIC result of that model. First, we established six demographic models based on different numbers of bottleneck events (Model-A to Model-F). The AIC results identify the preferred model for *J. microsperma* with two

bottlenecks (Model-E), and for *J. erectopatens* a model with one bottleneck and one population contraction (Model-D). We merged the preferred demographic scenarios to form the optimal model for the demographic history of *J. microsperma* and *J. erectopatens*. While fixing the merged demographic models, we further incorporate different divergence time and bottlenecks possibilities in the models to clarify the divergence time and bottleneck time of the two species. Based on Model-3 (the preferred model), we added bidirectional gene flow on it and considered different time possibilities of gene flow disappearance. The results preferred Model-3-5 as the best model for expounding the demographic history of *J. microsperma* and *J. erectopatens*.